A Scoping and Consensus Building Model for Understanding the Dynamics of a Blue-Green Algae Bloom

Steven Arquitt and Ron Johnstone
Centre for Marine Studies
University of Queensland
Brisbane QLD 4072 Australia
Telephone: 61 7 3365 4333
Facsimile 61 7 3365 4755
Email: sarquitt@mailbox.uq.edu.au
Email: rnje@mailbox.uq.edu.au

Abstract

So called nuisance blooms of Lyngbya majuscula have been occurring with increasing frequency in tropical coastal waters around the world. Outbreaks of this cyanobacterium (blue-green algae) threaten water quality, coastal ecosystems, and can be harmful in instances of human contact. While scientific and popular theories abound regarding lyngbya bloom initiation and growth, a clear research agenda has not emerged. In keeping with the modelling approach suggested by Costanza and Ruth (1997), this paper offers a scoping and consensus building model for the development of research directions. Development of this initial model is reported here as are simulation results that are instrumental in setting priorities for empirical investigations and future simulation-based research. It is expected that this preliminary model, after additional empirical work is completed, will lead to research and management models that will help set policy for community response to Lyngbya blooms.

Keywords

Lyngbya majuscula, algae bloom, system dynamics, scoping, consensus building

Introduction

Costanza and Ruth (1997) propose a three-stage modelling process for improving understanding and management of complex environmental systems. These three modelling stages include a *scoping and concensus building model* of low information resolution and high generality, a *research model* incorporating detailed historical or empirical data for the particular system of interest, and a *management model* building on the first two stages and used to examine the implications of management actions. We adopt this three-step modelling approach to address nuisance blooms of lyngbya majuscula, a filamentous cyanobacterium (blue-green algae), which have been occurring with increasing frequency over the past decade in tropical and sub-tropical coastal marine waters. This paper presents our efforts in the first stage of the three step modelling process, i.e., the development of a scoping and consensus building model.

Lyngbya occurs naturally at low densities in coastal marine environments in tropical and sub-tropical regions but has the potential to irrupt in massive blooms, which can adversely impact human health, the natural environment and local economies. The blooms have been observed

to cover areas of over 8 km^2 within a period of days and can persists for several months (Dennison et al 1999, Watkinson 2000). The cause of the blooms is not well understood and is the primary focus of the first stage of our modelling project.

A number of dynamic models have examined management policies for algae and cyanobacteria blooms. Anderson's (1973) classic system dynamics model of algae and eutrophication, and recent work by Pei and Ma (2002) on nutrient limitation on algae growth in lakes are two examples. Our objective in the first stage is to develop a conceptual model of lyngbya bloom causation based on the existing literature and incorporating the fieldwork and empirical research of marine scientists working on the lyngbya bloom problem. The first stage model will serve as a forum for refutation and consensus building and will help guide a strategic research agenda through the identification of sensitive or uncertain parameters and structures of key significance, thus establishing the foundation for the development of the second stage research model. Our ultimate goal is the development of a management strategy to mitigate or eliminate lyngbya blooms through policy analyses and design based on a management model.

The next section describes the *lyngbya* bloom problem. We then present our dynamic hypothesis of bloom causation, which provides the conceptual framework for the first stage model. We follow with a discussion and analyses of the model behaviour. We conclude with a discussion of the implications of the model behaviour for setting a strategic research agenda and the development of the second stage research model.

Problem description

Lyngbya majuscula, popularly known as "fireweed," is a toxic filamentous cyanobacteria found worldwide in tropical and sub-tropical marine environments (Osborne et al 2000). Normally lyngbya is present in trace amounts as fragments in the coastal marine sediments, however, under certain conditions lyngbya can bloom explosively. Lyngbya blooms have been observed in Morton Bay, Queensland, Australia to cover an area of over 8 km^2 within a period of several days. The blooms can persist for periods of 3 to 6 months and are usually followed by rapid decline (Dennison et al 1999, Watkinson 2000). The cause of lyngbya bloom collapse is unknown, however there is evidence that viral attack may be responsible (Hewson 2001). Lyngbya is biphasic, exhibiting both a benthic and surface-floating form. During bloom episodes lyngbya forms thick mats on the seafloor, often growing over and damaging seagrasses or other macrophytes. Masses of lyngbya biomass can float to the suface when gas bubbles become trapped in the filaments during periods of rapid photosynthesis (O'Neal et al 2000). Floating lyngbya washes ashore befouling coastlines with large amounts of decaying beach wrack. Lyngbya reproduces by means of fragmentation and it is thought that the floating phase is important in dispersal of filament fragments through the environment (Beer 1986).

Adverse impacts of lyngbya blooms

Lyngbya blooms can have significant adverse impacts on human health, coastal ecosystems, and local economies. Lyngbya has been associated with acute contact dermatitis and eye and respiratory infections in humans (Dennison et al 1999). In particular recreational swimmers and those working in the fishing industry are at risk. Moreover, three toxins isolated in lyngbya are known tumor promoters (Osborne et al 2000). There is evidence that lyngbya causes seagrass loss when seagrass beds are overgrown (Dennison et al 1999). Seagrass beds

are key habitat for many marine species including dugongs and green sea turtles, both rare and endangered species. There are also reports of reduced catches of fish and crabs during bloom years (Watkinson 2000). Work by O'Neal at al (2000) indicates that lyngbya bloom may cause nitrogen loading through nitrogen fixation and detrital decay leading to localized eutrophic conditions. During bloom events local economies suffer through damaged commercial and recreational fisheries and diminished recreational value of effected areas due to perceived health risks and loss of aesthetic appeal. Floating lyngbya mats washed ashore necessitate cleanup programs. Local governments are under pressure to eradicate lyngbya blooms and are investing in expensive programs to physically remove lyngbya from the environment and are now prompted to invest in research programs to better understand why lyngbya blooms occur and how they may be controlled or eliminated.

Dynamic hypothesis

Growing evidence indicates that lyngbya growth may be limited by bioavailable iron, and that increases in bioavailable iron are linked to the blooms (Dennison et al 1999, Gross 1996). Iron is one of the most abundant elements on earth, however its bioavailablity is strongly dependent on its speciation (Watkinson 2000). Ferrous iron, Fe (II), which exists under anoxic conditions, is bioavailable and found in the anoxic layer of the coastal marine sediment. Ferrous iron effluxes into the water column from the sediment porewater if the overlying water becomes anoxic. Under oxic conditions ferrous iron very rapidly oxidizes to insoluble oxyhydroxides which are not bioavailable (DiToro 2001). A second category of bioavailable iron comprises organically-bound iron complexes associated with humic or fulvic acids (Matsunaga et al 1998). These organically-bound iron complexes originate on land and enter the coastal marine environment through surface runoff and groundwater discharge. The organically-bound iron complexes remain bioavailable under oxic conditions and have been shown to be important sources of iron for planktonic algae (Matsunaga et al1998).

A preliminary hypothesis has emerged which suggests that lyngbya blooms occur in response to a pulse of bioavailable iron entering the coastal marine environment during periods when conditions of light and temperature are in the optimal range for lyngbya growth (Watkinson 2000). The pulse originates from anthropogenic land cover alterations, such as forest felling in areas of humic soils which cause runoff of organically-bound iron complexes during heavy rain events. The pulse of bioavailable iron overrides the normal iron limitation on lyngbya growth and lyngbya begins to grow at a compounding rate. When lyngbya biomass increases, respiration and detritus decay also increase. The dual influence of respiration and detrital decay drive down the night levels of dissolved oxygen. The lowered level of dissolved oxygen during nights triggers efflux of ferrous iron from the sediment during nights, which in turn increases bioavailable iron and lyngbya growth, allowing the bloom to persist for a period of months even after the initial pulse of organically-bound iron has dissipated. Eventually the growth of lyngbya biomass will level off as the carrying capacity for lyngbya is approached.

It is this hypothesis which we intend to elaborate and explore through the development of a dynamic scoping and consensus building model. Figure 1 below is a causal loop diagram which shows the feedback structure of our dynamic hypothesis. This feedback structure provides the focus for the development of the formal system dynamics model which follows.
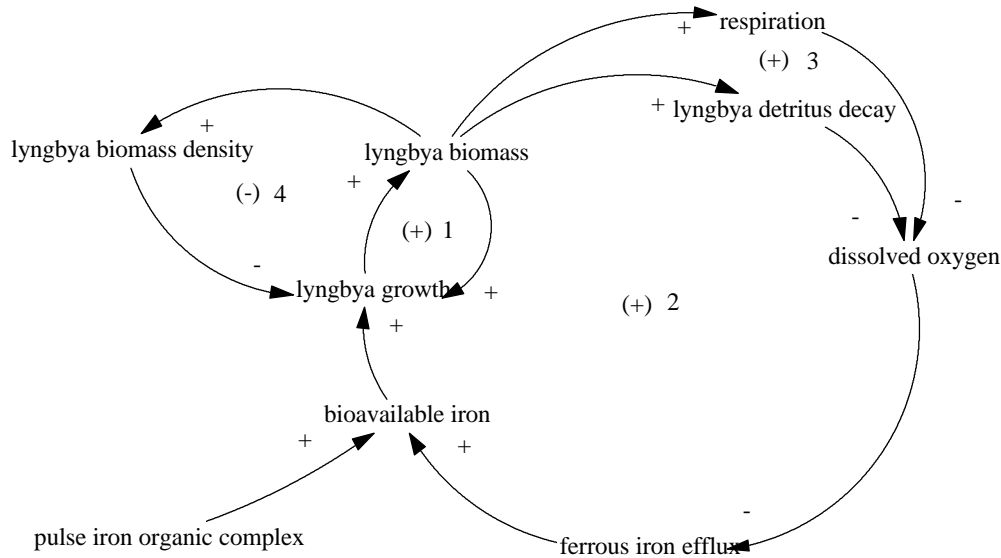
Figure 1. Causal loop diagram for dynamic hypothesis of lyngbya bloom
(For the sake of clarity less important feedbacks have been omitted.)

We hypothesize that lyngbya bloom is caused by 3 major positive feedback loops: Loop 1 in the diagram above, which compounds the growth of lyngbya, and Loops 2 and 3 which increase the availability of lyngbya's limiting resource, bioavailable iron. A negative feedback loop, Loop 4, limits the growth of lyngbya through the influence of the environmental carrying capacity. The carrying capacity is based on field observations and is considered to be the maximum density of lyngbya possible in the study area due to limiting effects of other nutrients, self-shading, disease, etc. A shift in dominance from the positive feedback loops causing growth to the negative loop linked to the carrying capacity creates a dynamic pattern of s-shaped growth. This accords with our reference mode which is initial exponential growth of lyngbya biomass followed by a period of slower sustained growth. We do not concern ourselves at this stage with the eventual collapse of the blooms. We now turn to a description of the formal system dynamics model.

Model structure

General structure

Our model consists of four interacting sectors, the *Lyngbya Sector*, the *Iron Sector*, the *Dissolved Oxygen Sector*, and the *Seagrass Sector*. The Seagrass Sector has been included because of the important role of seagrass in the dissolved oxygen balance of the ecosystem and because seagrass meadows are the foundation of a diverse ecological community adversely impacted upon by lyngbya blooms. The stocks in the Lyngbya, Dissolved Oxygen and Iron Sectors are modelled as arrays. The arrays consist of two elements, upper and lower, to represent distinct system behaviours in the upper and lower water columns. These sectors could have been built with non-arrayed stocks, however we found that the cognitive maps without the arrays quickly became visually intractable. The Seagrass sector is built without making use of arrays. This is because seagrasses are benthic species with very little drifting

biomass in the upper water column. In our model seagrasses directly interact with the lower water column only.

Our model is generic but is parameterised to correspond roughly with study areas in southeast Queensland, Australia where lyngbya blooms have been and are a continuing problem. The generic study area is 10 km^2. The water depth is 2 meters, upper and lower water column each being one meter in depth. Our step size is one half-day to allow us to represent the diurnal processes of carbon uptake and respiration and the key influences of these on the patterns of dissolved oxygen and bioavailable iron. The half days represent day and night alternately. We use a switch based on a sinwave function to switch day and night processes, i.e., carbon uptake and respiration, on and off. We run our simulations over a period of 180 half days, or three months.
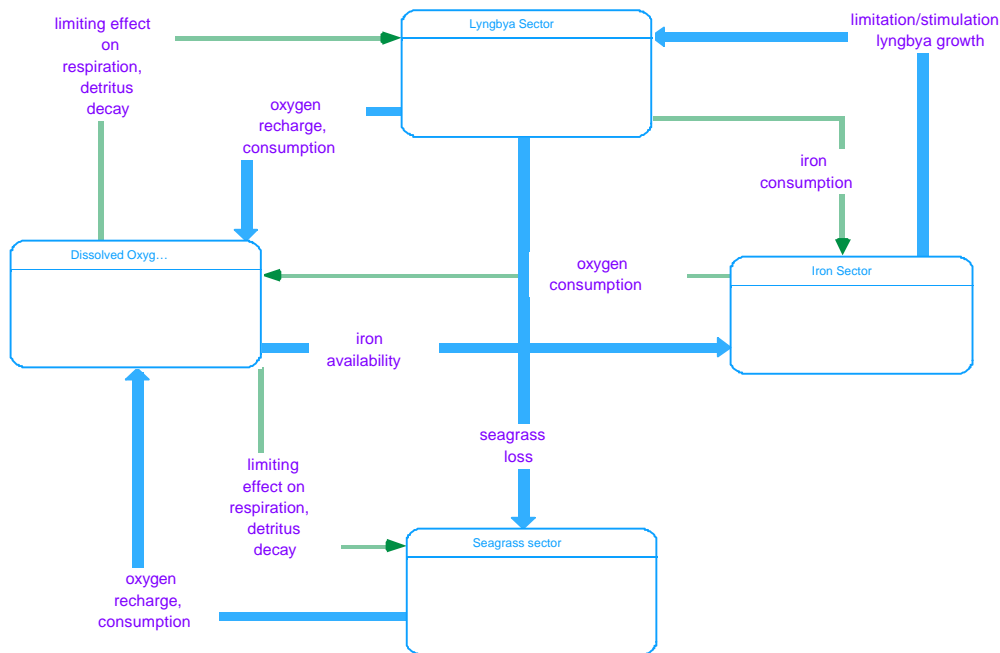

Figure 2. Principal interactions between sectors

The diagram above shows the principal interactions between the sectors. Thick lines indicate major influences, thin line less significant influences. The Lyngbya and Seagrass sectors strongly influence the level of dissolved oxygen through carbon uptake, respiration, and detritus decay. The Dissolved Oxygen sector feeds back to the Lyngbya and Seagrass sectors by modifying respiration and detritus decay through oxygen limitation. The Dissolved Oxygen sector has a strong influence on the level of bioavailable iron through its effect on ferrous iron efflux. The iron sector has a moderate feedback to the oxygen sector through the consumption of oxygen by oxidation of ferrous iron. The iron sector strongly influences the lyngbya sector through the effect of bioavailable iron concentration on lyngbya growth. The lyngbya sector consumes a fraction of the iron in the process of growth. The Lyngbya Sector effects the seagrass sector by reducing seagrass biomass through overgrowth and shading.

The following sections describe the structure of the individual sectors. The first paragraph gives a brief description of the sector. This is then followed by a detailed sector description. Full model equations are given in the appendix.

Lyngbya sector

Figure 3 shows the stock and flow structure of the Lyngbya Sector. The Lyngbya Sector represents the growth of carbon biomass by means of an exogenous maximum carbon uptake rate fraction modified by two limiting factors, bioavailable iron and carrying capacity. Both limiting factors are based on empirical data and exert their effects through non-linear graph functions. Respiration and detritus decay are modelled as flows based on rate fractions influenced by an oxygen limitation factor. The transition of Lyngbya biomass to the floating phase is modelled as a function of carbon uptake. Loss of biomass and detritus through drift are based on drift times which differ for the upper and lower water column. Lyngbya respiration and detritus decay are linked to the Dissolved Oxygen Sector where they contribute to oxygen consumption and anoxia. The influence of anoxia and, in turn, the concentration of bioavailable iron, completes the positive feedback loop which drives lyngbya bloom.
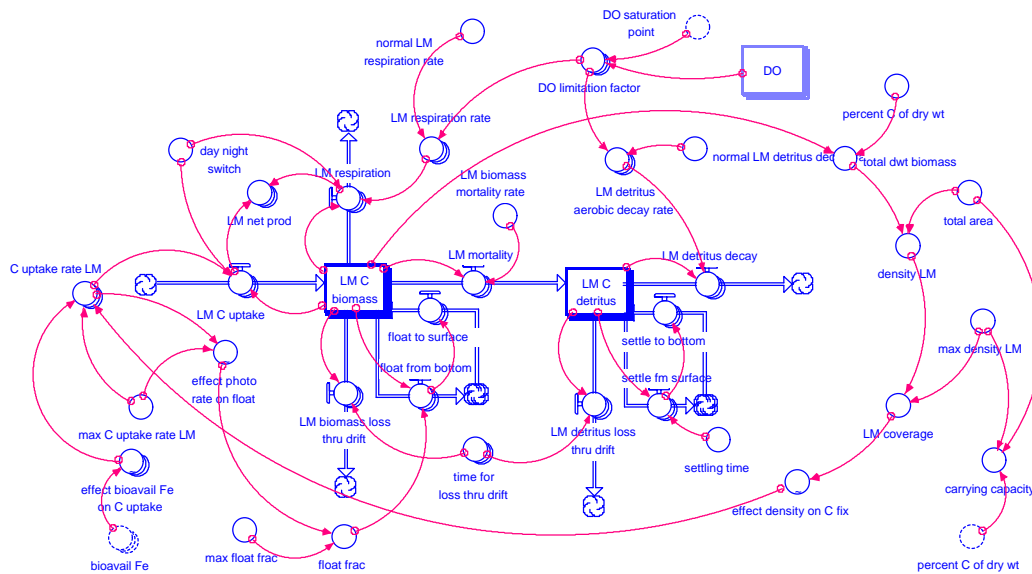

Figure 3. Lyngbya Sector

The Lyngbya Sector includes two arrayed stocks, lyngbya carbon biomass *LM C biomass* and lyngbya carbon detritus *LM C detritus*. We have chosen to model carbon in lyngbya for two reasons: (i) empirical data for biomass, growth rates, and detritus decay are often expressed in carbon terms and, more importantly, (ii) carbonaceous oxygen consumption through respiration and detritus decay has important effects on dissolved oxygen and concentrations of bioavailable iron. Carbon is considered to be non-limiting in our model. *LM C biomass* is modelled with an array in order to represent its biphasic nature. *LM C biomass upper* represents floating lyngbya biomass and *LM C biomass lower* represents benthic lyngbya biomass. The array facility is used in the same fashion to model floating and benthic *LM C*

detritus.   The two arrayed stocks represent the total mass in grams of carbon in lyngbya biomass and detritus within the generic study area.

Both upper and lower elements of the arrayed stock *LM C biomass* are fed by carbon uptake *LM C uptake*. Net production *net prod* is the difference between carbon uptake and respiration and serves as our surrogate for lyngbya biomass growth. We consider normal day respiration to be subsumed in carbon uptake. To derive *net prod* we subtract *LM respiration* from *LM C uptake* delayed by one time step.

The growth formulations used by almost all models of algae or cyanobacteria make use of a maximum growth rate at a particular temperature modified by functions for light and nutrient limitation (EPA 1985). In our model we are primarily concerned with endogenous variables, we therefore assume that temperature and light are within optimal ranges for the growth of lyngbya. Since we are modelling carbon biomass we make use of a maximum rate of carbon uptake *max C uptake LM* modified by the effect of bioavailable iron *effect bioavail Fe on C uptake* and a density dependent factor *effect density on C uptake* to yield a carbon uptake rate *C uptake rate LM*. To formulate the density dependent function we follow Ford's (1999) recommendations on modelling density-dependent relationships. *Effect density on C uptake* is a non-linear graphical function of lyngbya coverage which is the ratio of lyngbya biomass density and the maximum lyngbya biomass density expressed in grams dry weight. *Max LM density* is derived from field observations (Watkinson 2000) and is here considered to be the environmental carrying capacity for lyngbya. The conversion from carbon biomass to grams dry weight is made with a conversion factor which is assumed to be constant.

Models of nutrient limitation for algae and cyanobacteria fall into two major categories, fixed stoichiometry and variable stoichiometry models (EPA 1985). Fixed stoichiometry models define nutrient uptake based on the average elemental ratio found in the species under study and operate under assumptions that the elemental composition of the species is invariant. Variable stoichiometry models account for separate processes of nutrient absorption from the environment and assimilation into biomass as described by Hannon and Ruth (1997) and followed by Pei and Ma (2002) in their recent work on algae fluctuations in lakes. Variable stoichiometry models implicitly assume that the algae or cyanobacteria has the ability to store the nutrient in question and can continue to grow by drawing on nutrient reserves even when external nutrients are depleted (EPA 1985). Work done by Gross and Marten (1996) indicates that lyngbya majuscula may have little or no capacity to store reserves of iron. Based on this assumption we have adopted a fixed stoichiometry approach for our model.

Typically, fixed stoichiometry models are based on Michaelis-Menton kinetics in which the growth rate is expressed as:

$$U = umax*\{c/(K + c)\}$$

Where umax is the intrinsic maximum rate of growth, K is the half-saturation constant for the limiting nutrient, and c is the external concentration of the limiting nutrient (EPA 1985). Despite its wide acceptance and use we have found that the Michaelis-Menton equation does not lend us the flexibility to accurately capture the relationship between bioavailable iron concentration and lyngbya growth. As an alternative approach to the concentration-growth formulation we have used empirical data from the research of Gross and Martin (1996) to build a graphical function expressing the effect of bioavailable iron concentration on carbon uptake including inhibitory effects above optimal concentrations.

LM C biomass is drained by respiration *LM respiration* and lyngbya mortality *LM mortality*. The respiration rate is the product of normal respiration rate and the dissolved oxygen limitation factor *DO limitation factor*, following Anderson's (1973) work on eutrophication in lakes. It has been postulated that the transition from benthic to floating biomass is a function of the rate of carbon uptake (O'Neil et al 2000). The flow *float from bottom* mimics the transition from benthic to floating biomass. The *float fraction* is the product of an exogeneous maximum float fraction and the effect of the carbon uptake rate represented by the graphical function *effect C uptake rate on float*. The inflow *float to surface* is set equal to *float from bottom* and is necessary to account for the flow from the lower element of the arrayed stock to the upper. Some lyngbya floating biomass will be lost from the system through drift to waters outside the study area or will be washed ashore as beach wrack. Some benthic biomass will also be washed out of the system, albeit at a slower rate. These processes are represented with the arrayed flow *biomass lost thru drift*.

Lyngbya mortality transfers carbon from the stock of lyngbya biomass to the stock of lyngbya carbon detritus *LM C detritus*. For our purposes we only consider aerobic detritus decay, which we represent with the flow *LM detritus decay*. Following Anderson's (1973) work the aerobic rate of decay is modified by the *DO limitation factor*. Floating detritus will settle relatively quickly and accumulate on the benthic surface. We model this process with the flow *settle to bottom*. *Settle from top* completes the flow between the two elements. Similarly to the case with biomass, we model the loss of detritus through drift with the *flow LM detritus loss thru drift* with the surface loss occurring much more rapidly than benthic.

Dissolved Oxygen Sector

The Dissolved Oxygen Sector models processes which influence the levels of dissolved oxygen in the upper and lower water columns. The level of dissolved oxygen is influenced by carbon uptake, respiration, and detritus decay of lyngbya and seagrass and by water exchange. The dissolved oxygen level of the lower water column has a key influence on bioavailable iron levels in the Iron Sector and, hence on the growth rate of lyngbya.
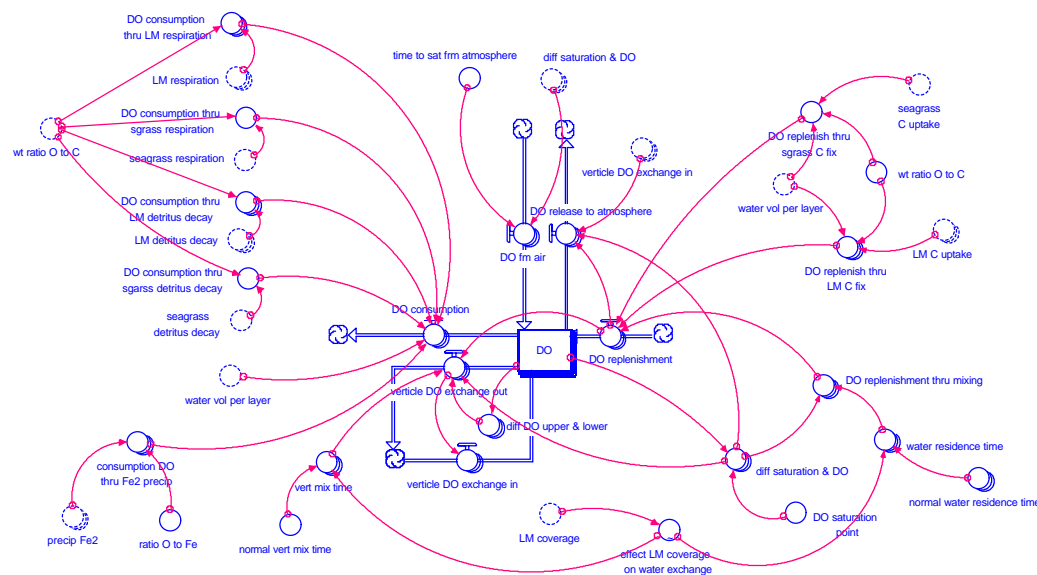
Figure 4. Dissolved Oxygen Sector

The dissolved oxygen sector contains one arrayed stock representing the concentration of dissolved oxygen *DO*. The array contains two elements, one representing the concentration of dissolved oxygen in the upper water column *DO upper* and one representing the concentration in the lower water column *DO lower*. The units are grams elemental oxygen per m^3. Reoxygenation occurs through carbon uptake and corresponding oxygen release of lyngbya and seagrass and through mixing with oxygenated waters from outside the study area. These reoxygenation processes are represented by the flow *DO replenishment*. Reoxygenation through carbon uptake to *DO upper* includes reoxygenation from floating lyngbya only. Reoxygenation from benthic lyngbya and seagrass replenish *DO lower*. Both DO upper and DO lower are replenished by mixing *DO replenishment thru mixing*. We assume that seawater outside the study area is saturated with oxygen and that both upper and lower layers tend toward oxygen saturation at a rate defined by the *water residence* time and the difference between *DO* and oxygen saturation. Oxygen consumption occurs through respiration and detrital decay of both lyngbya and seagrass. To convert carbon uptake, respiration, and detritus decay from carbon to oxygen terms, we use the stoichiometric ratio 2.67 moles oxygen to one mole carbon.

DO upper and *DO lower* are linked by a mass balance structure *vertical DO exchange out* and *vertical DO exchange in* which tends to equilibrate the upper and lower dissolved oxygen values over the time period *vertical mix time*. During periods of rapid photosynthesis there will be a tendency toward supersaturation of oxygen in the water column and dissolved oxygen will rapidly bubble away to the atmosphere. Given the rapid nature of this flow we have linked it directly to the inflow *DO replenishment*; when *DO lower* exceeds the saturation point, the flow to *DO upper* becomes equal to *DO replenishment lower*. When *DO upper* exceeds the saturation point the flow *DO release to air* becomes equal to *DO replenishment*. Our model only considers dissolved oxygen exchange between the upper and lower water columns through mixing. In reality, there is also some dissolved oxygen exchange occurring through diffusion. We choose to ignore the diffusion process because it is very slow compared to reoxygenation through carbon uptake and water exchange and is unlikely to significantly influence the model behaviour. The upper water column will be reoxygenated through diffusion from the atmosphere. We have added a flow *DO from atmosphere* to mimic reoxygenation from the atmosphere into the upper water column. This flow is defined by the difference between *DO upper* and the saturation point modified by a time to reach saturation *time to sat fm atmosphere*.

The growth of thick lyngbya mats on the benthic surface restricts the exchange of water vertically and laterally at the sediment-water interface. Due to the restricted water exchange dissolved oxygen will reach lower and higher levels at night and day respectively. To mimic the effect of lyngbya coverage on water exchange we have linked lingbya coverage *LM coverage*, which is the ratio of lyngbya density to maximum lyngbya density, to water residence time for the lower water column and to the vertical mixing time with a non-linear function. As lyngbya coverage increases the vertical mixing and water residence times will increase.

The iron sector

The iron sector models the processes behind the bioavailability of iron. Bioavailable iron takes two forms (i) the group of organically-bound iron complexes from land based sources

and (ii) ferrous iron which originates from the marine sediment. The organically-bound iron enters the marine environment as a base flow which we consider to remain constant and as a pulse which represents massive entry associated with a rain event. Ferrous iron enters the environment by efflux from the sediments and is dependent of the concentration of dissolved oxygen in the water column. Under oxic conditions ferrous iron is not available, under anoxic conditions ferrous iron efflux occurs. The concentration of bioavailable iron is the key factor in our hypothesis of lyngbya bloom.

Figure 5. Iron Sector

The iron sector contains 2 arrayed stocks representing the concentrations in the water column of the two classes of bioavailable iron, organically-bound iron compounds *Fe complex* and ferrous iron *Fe2*. The units for the stocks are grams per m^3. The stocks are arrayed into upper and lower elements to represent distinct processes in the upper and lower water column.

In our model the uptake of bioavailable iron by lyngbya *uptake bioavail Fe* is based on net production, the difference between carbon uptake and carbon loss through respiration. We assume that bioavailable iron is taken up at a rate equal to net production converted from carbon to iron by a fixed stoichiometric ratio. We further assume that *Fe complex* and *Fe2* are taken up at equal per unit rates. We account for the equivalent uptake rates through proportionality factors *Fe complex to bioavail Fe* and *Fe2 to bioavail Fe,* which are the ratios of *Fe complex* and *Fe2* to their sum *biovail Fe*.

Iron complex enters the generic study area through surface runoff and groundwater flux. *Fe complex upper* and *lower* is fed by *inflow Fe complex from land* which includes a base flow of iron complex *baseflow Fe complex*, which we assume remains constant, and *pulse Fe*

complex which mimics a massive influx of organic iron complex associated with a rain event. *Pulse Fe complex* is expressed using a graphical function over time. We use a first order exponential smooth function to mimic the dispersion of the pulse throughout the study area. Another source of iron complex is iron reintroduced to the environment through detrital decay of lyngbya *Fe reintroduction*. We represent this with a co-flow of *LM detritus aerobic decay* multiplied by a conversion factor to convert from carbon to iron. Again, we assume that this ratio is constant. The extent to which iron from detrital decay is bioavailable is uncertain. For this reason we modify the flow *Fe reintroduction* with a bioavailability fraction *frac reintroduced Fe bioavail* with which we can experiment. *Fe reintroduction* is linked to the detrital decay flows via the array. *Fe reintroduction upper* arises from the decay of floating lyngbya detritus, *Fe reintroduction lower* arises from benthic detritus. The coupled flows *Fe complex vert mix out* and *Fe complex vert mix in* represent vertical mixing between upper and lower layers of *Fe complex* in identical fashion to the structure for vertical mixing in the Dissolved Oxygen Sector. An identical structure is used to account for vertical mixing of *Fe2*. Two additional flows drain *Fe complex*. We assume that the organic iron complexes will decay at some average rate into forms not bioavailable. We model this process with the flow *decay Fe complex,* which is *Fe complex* divided by an average lifetime. Some iron complex will be lost from the study area through mixing with surrounding waters. This is accounted for by *Fe complex loss due water exchange,* which *is Fe complex* divided by the water residence time. An identical structure is used to account for loss of *Fe2* through water exchange.

The source of ferrous iron *Fe2* is the sediment. When dissolved oxygen approaches anoxic levels Fe2 will efflux from the sediment. In the presence of dissolved oxygen ferrous iron rapidly oxidizes to form non-bioavailable iron oxyhydroxide compounds which precipitate back to the sediment. In our model the biflow efflux Fe2 is formulated based on Fick's Law of diffusion. Fick's Law states that the mass of a solute crossing a unit area per unit time is proportional to the gradient of concentration of the solute (DiToro 2001). We formulate *indicated efflux Fe2* by multiplying the difference in concentration of Fe2 in the sediment and water column by a diffusion coefficient and by a value for the porosity of the sediment expressed as the fraction of porewater in sediment (DiToro 2001). We assume that the concentration of Fe2 in the sediment remains constant. This assumption seems reasonable given the ongoing production of Fe2 in the anoxic layer of the sediments through reduction of iron oxyhydroxides from sedimentation and precipitation from oxidation of Fe2 in the water column. Bioturbation, the sediment churning action of benthic organisms, can significantly increase solute efflux (Hoffman). We account for this with a *bioturbation factor* which is multiplied by the diffusion coefficient.

The influence of dissolved oxygen on ferrous iron efflux *efflux Fe2* is exerted through a graph function of the dissolved oxygen concentration in the lower water column *DO lower* over the oxygen saturation point. This is multiplied by *indicated Fe2 efflux* to give the biflow *efflux Fe2*. We use a biflow to allow reverse flux into the sediment in the case of reversal of the Fe2 concentration gradient. Under oxic conditions ferrous iron has a very short lifetime in the water column, on the order of seconds, before precipitating as iron oxyhydroxide. We mimic the precipitation of Fe2 through the flow *precip Fe2*. Our precipitation time is defined as a non-linear function of the dissolved oxygen concentration *DO* over the oxygen saturation point. During daylight the water column will become strongly oxic due to the effects of carbon fixation and the precipitation time for Fe2 will become very short. Due to our selection of time dimension and step size we are unable to simulate processes on the order of

seconds in our model. However, as we believe it important to explicitly model the precipitation of Fe2, we set our minimum precipitation time as DT*3.

Seagrass sector

We include a seagrass sector in our model because seagrass is a key ecosystem component adversely impacted upon by blooms of lyngbya. Field studies indicate that lyngbya blooms can reduce seagrass biomass through overgrowth and shading. Seagrass regenerates slowly and there is concern that recurrent blooms of lyngbya could seriously deplete seagrass stocks. The seagrass uses the same basic structure for growth, mortality and detritus decay dynamics as the Lyngbya Sector. A graph function based on lyngbya coverage mimics the impact of lyngbya on seagrass by reducing the seagrass carbon uptake rate.
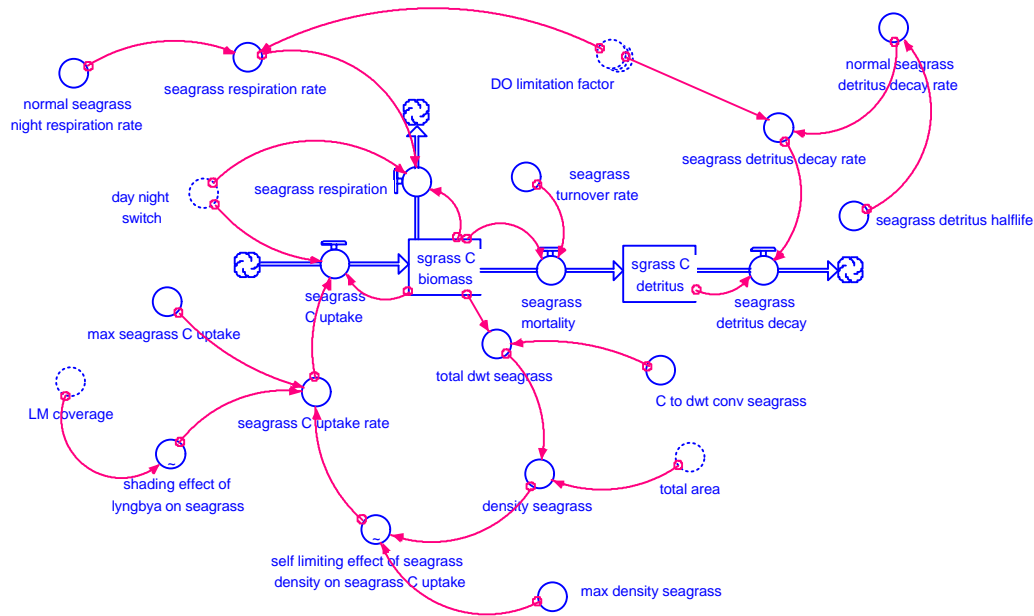
Figure 6. Seagrass Sector

The seagrass sector contains two stocks, seagrass carbon biomass *sgrass C biomass* and seagrass detritus *sgrass C detritus*. *Sgrass C biomass* represents total carbon of seagrass above and below the sediment surface. *Sgrass C biomass* represents the total carbon in seagrass detritus. Because seagrass is a benthic life form without a significant amount of mass taking a surface floating form we use non-arrayed stocks to represent seagrass biomass and detritus. We assume that seagrass directly influences dissolved oxygen in the lower water column only.

The seagrass model structure is similar to that for lyngbya. The *seagrass C uptake rate* is the *max seagrass C uptake rate* multiplied by a graph function representing the harmful effect of lyngbya overgrowth on seagrasses *shading effect of lyngbya on seagrass* and a density-dependent factor represented by a graph function *self limiting effect of seagrass density on seagrass C uptake*. The density-dependent factor is a function of the ratio of seagrass density to maximum seagrass density and represents the effect of the carrying capacity of seagrass. We do not consider iron to be a limiting factor for seagrass and hence do not link external bioavailable iron concentration to the carbon uptake rate for seagrass. Lyngbya carbon

biomass is drained by *seagrass respiration* and *seagrass mortality*. As in the Lyngbya Sector, we assume that day respiration is subsumed in carbon uptake, i.e., that carbon uptake is total carbon uptake minus day respiration. *Seagrass respiration* is modified by the *DO limitation factor* as in Lyngbya Sector. *Seagrass mortality* is formulated with an exogenous mortality rate. *Seagrass C detritus* decays based on a decay rate that is influenced by the *DO limitation factor*.

Model behaviour

Base simulation

Figures 7a and b display our base simulation which approximates the basic pattern of our reference mode, i.e., a short period of rapid growth followed by slower sustained growth.
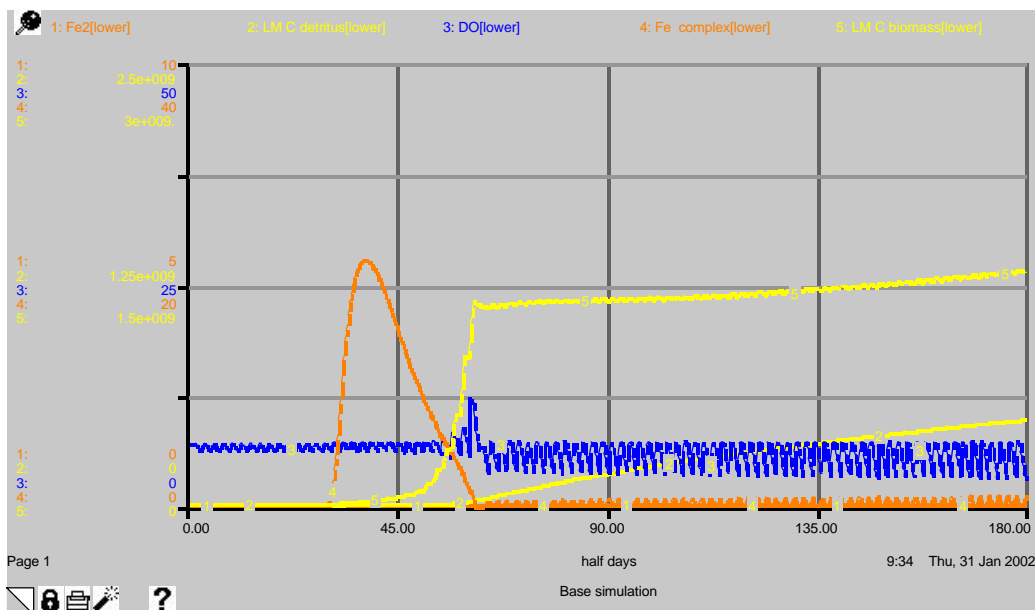
Figure 7a. Base simulation
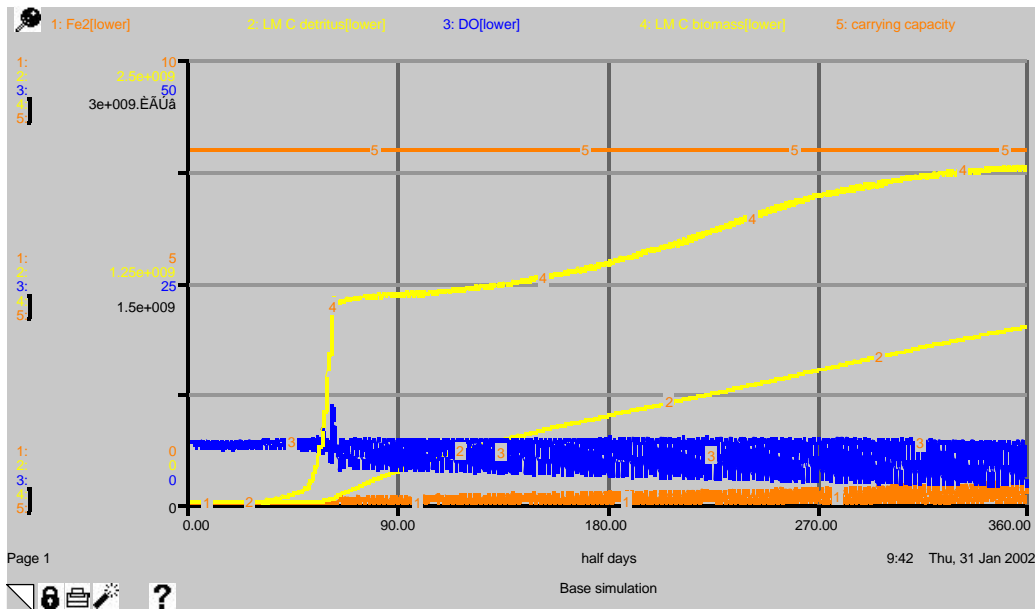
Figure 7b. Base simulation
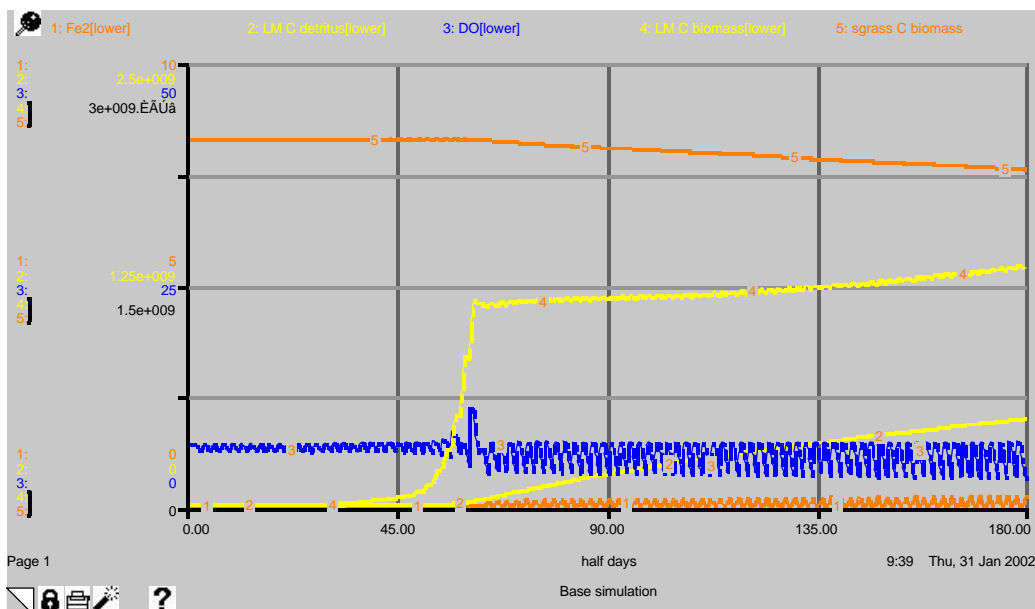
Figure 7c. Base simulation

The simulation is initially set in equilibrium. From time zero DO oscillates due to the diurnal effect of seagrass on dissolved oxygen through carbon uptake and respiration. At time 30 a pulse of iron complex enters the coastal waters. Lyngbya enters a phase of rapid exponential growth in response. By time 70 the pulse of iron complex has disappeared due to dissipation through water exchange and consumption by lyngbya. However, the great increase in lyngbya biomass accelerates respiration and detritus decay which drive night dissolved oxygen down to lower levels causing efflux of Fe2 from the sediment. With Fe2 providing the bioavailable iron, lyngbya contiues to grow at a slower rate after the pulse of iron complex has dissipated. Fe2 oscillates because its efflux occurs at night only. During the day Fe2 is rapidly oxidized and precipitates as oxyhydroxide. DO briefly becomes supersaturated around time 70 due to

the high rate of carbon uptake during the near vertical growth of lyngbya biomass. Lyngbya detritus begins to increase at time 70 and contributes to dissolved oxygen consumption. Figure 7b is simulated over a period of 6 months. We see that lyngbya biomass actually follows a two-phase pattern of growth, an initial phase of rapid exponential growth based on Fe complex, followed by a slower growth period based on Fe2. Biomass approaches its carrying capacity asymptotically. Figure 7c demonstrates the impact of lyngbya growth on seagrass biomass which begins to decline slowly as lyngbya coverage increases .

Simulation of our reference mode lends us a degree of confidence in our first-stage model structure. We now go on to explore the model's behaviour through sensitivity analysis of parameters and structures.

Sensitivity analysis

Many of the parameters and structures in the model are highly uncertain. Nevertheless, they are considered important to system behaviour and hypothesis development and are therefore not excluded. Uncertain parameters which are sensitive to system behaviour are candidates for further empirical research. In this way we use sensitivity analysis to focus our data acquisition needs and empirical research efforts for the development of our second-stage research model.

In the following sections we examine the sensitivity of lyngbya bloom to changes in various parameters and structures. We follow Sterman's (2000) guidance in analysing the sensitivity of combinations of parameters and structures as well as single parameters. We use lyngbya biomass in the lower water column as our measure of lyngbya bloom response. For each sensitivity run we give a brief explanation of the model behaviour and the insight it lends for the direction of further research needs.

Lyngbya Sector

Sensitivity of maximum carbon uptake rate for lyngbya *(Max C uptake rate LM)*
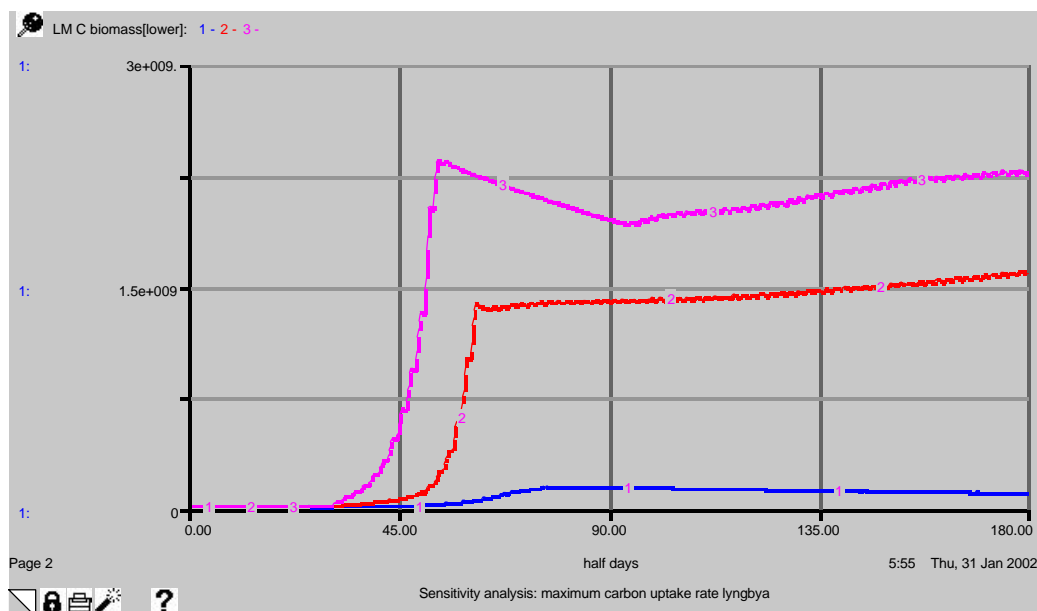
Figure 8. Sensitivity analysis of maximum lyngbya carbon uptake rate

Parameter settings for sensitivity analysis (fraction day⁻¹)			
Parameter	Setting 1	Setting 2 (base)	Setting 3
Max C uptake LM	.2	.5	1

The maximum carbon uptake rate is a key parameter in the formulations for growth of lyngbya biomass. As figure 8 demonstrates, maximum carbon uptake rate is a sensitive parameter. Maximum growth rates for cyanobacteria in the literature range from .2 to almost 5/day (EPA 1985). We have selected .5 for our base run. More realistic formulations for lyngbya bloom growth will require a more accurate range of maximum carbon uptake rate for lyngbya. Based on our sensitivity analysis, we identify the maximum carbon uptake rate as an important research priority.

Sensitivity of Lyngbya respiration and mortality rates *(normal LM respiration, LM mortality rate)*

Values for respiration and mortality of cyanobacteria and green algae vary widely (EPA 1985). No values for respiration and mortality rates for lyngbya are known from the literature. At equilibrium respiration and mortality must equal carbon uptake. In the flowing sensitivity analysis we vary the ratios of respiration rate to mortality rate while holding their sum equal to the equilibrium rate of carbon uptake.
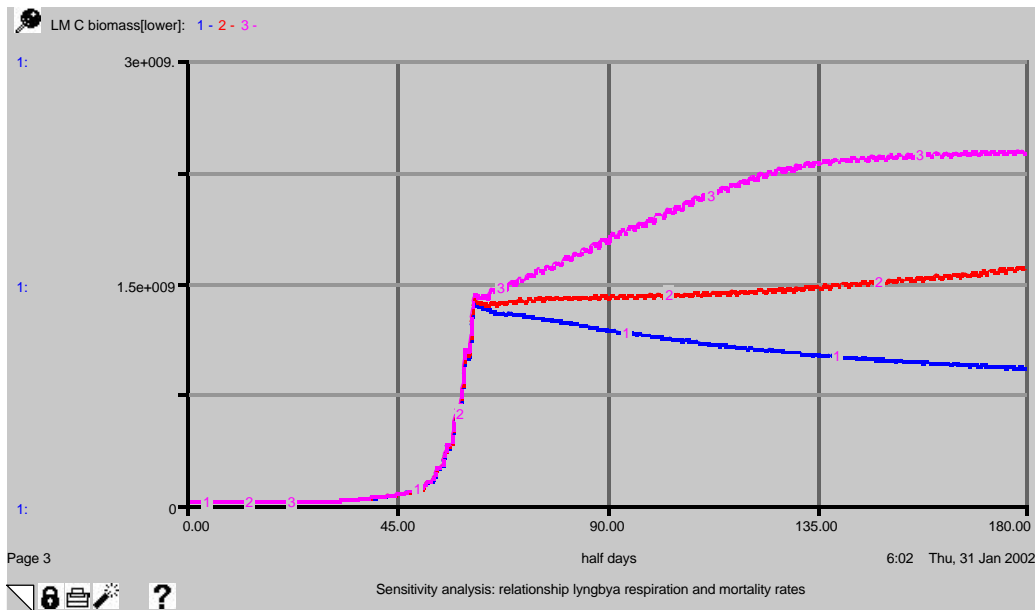
Figure 9. Sensitivity analysis of normal respiration and mortality rates

Parameter settings for sensitivity analysis (fraction day⁻¹)			
Parameter	Setting 1	Setting 2 (base)	Setting 3
Normal LM respiration rate	.001	.01	.019

LM mortality	.019	.01	.001

When the normal respiration rate is set at its lowest level lyngbya biomass begins to decline after the initial exponential growth phase. This is because the respiration rate is insufficient to drive down the night oxygen level to a level low enough to allow release of Fe2 from the sediment. *Caeterus paribus* this suggest that respiration is a more important factor in Fe2 efflux than is detritus decay. Setting 3 causes adequate Fe2 efflux for the lyngbya bloom to reach its full limit. Sensitivity analysis indicates that lyngbya respiration has very important influence on Fe2 efflux and, thus is an important focus for empirical research.

Sensitivity of lyngbya detritus decay rate *(normal LM detritus decay rate)*

Our initial hypothesis considers detritus decay to be an important factor in the creation of anoxic conditions which allow Fe2 efflux and continuance of lyngbya bloom. However, the detritus decay rate is a very uncertain parameter. We have used the value of .01/day in our base simulation for the purpose of setting the model into equilibrium.
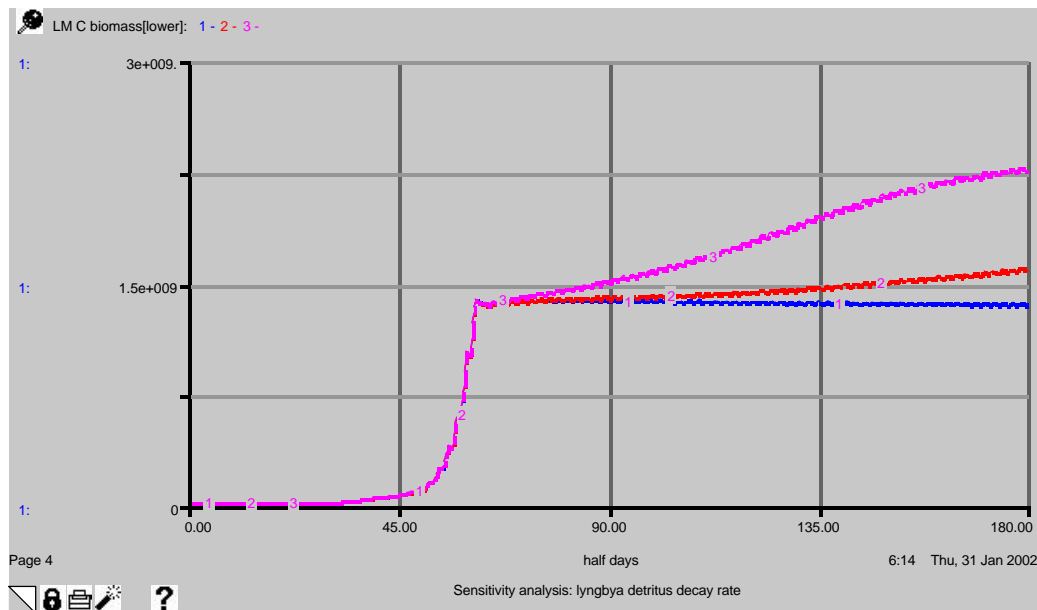

Figure 10. Sensitivity analysis of normal lyngbya detritus decay rate

Parameter settings for sensitivity analysis (fraction day^{-1})			
Parameter	Setting 1	Setting 2	Setting 3
Normal LM detritus decay rate	.001	.01	.1

Setting 3 allows lyngbya bloom to grow to a significantly higher level after the initial period of sharp exponential growth. This is because the increased rate of oxygen consumption associated with detritus decay causes more extreme anoxia in the water column. When the

detritus decay rate is set to a low level, as in setting 1, Fe2 efflux is just adequate to sustain a replacement rate of Lyngbya growth.

Sensitivity of relationships between detritus decay and respiration

Our hypothesis of lyngbya bloom states that detritus decay and respiration are important in perpetuation of the bloom. It is interesting to compare different combinations of detritus decay and respiration rates to try to understand which of the two is the more important determinant of lyngbya bloom perpetuation.
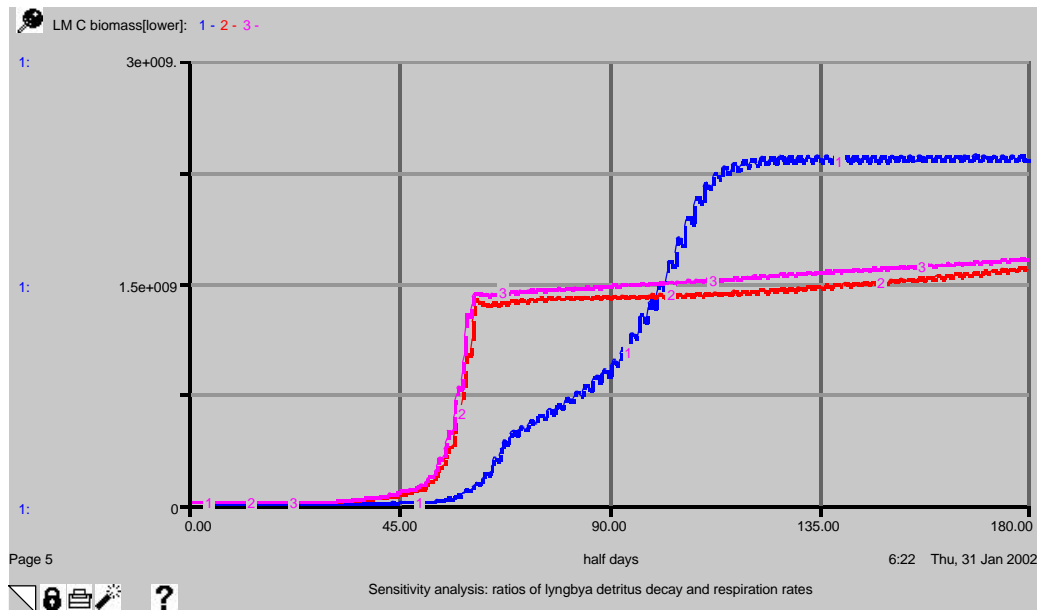
Figure 11. Sensitivity analysis of normal lyngbya detritus decay and respiration rates.

Parameter settings for sensitivity analysis (fraction day^{-1}, dimensionless)			
Parameter	Setting 1	Setting 2 (base)	Setting 3
Normal LM detritus decay rate	.001	.01	.1
Normal LM respiration rate	.1	.01	.001

The lyngbya biomass at setting 1 responds more slowly to the pulse of bioavailable iron but eventually climbs to a higher level than with the other settings. The growth response is slower because net production is lower at setting 1 due to the much higher respiration rate. Eventually, however, as the biomass accumulates, the higher respiration rate causes more extreme anoxia and consequently greater Fe2 efflux and lyngbya growth. The simulation at setting 3 is not unlike the base run. The message from this sensitivity run is that both detritus decay rate and respiration rate are important for an understanding of lyngbya bloom dynamics. The implications for hypothesis development are that respiration may be a more important causal factor in Lyngbya bloom than detritus decay.

Sensitivity of structure for endogenous mortality rate

As lyngbya density increases disease incidence or other factors may raise the mortality rate. We have made a graph function *effect of lyngbya coverage* which exponentially increases the mortality rate as lyngbya coverage increases. The effect is delayed by 7 days to mimic an incubation period.
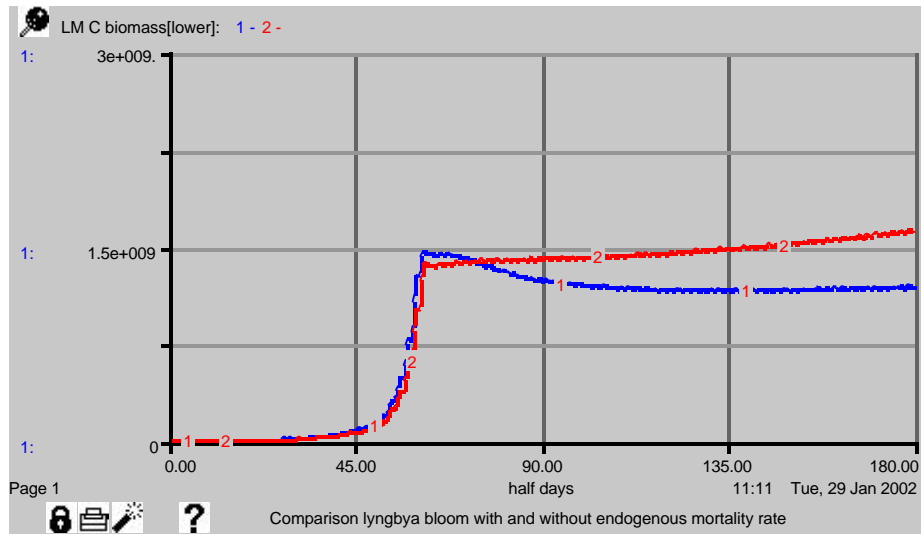

Figure 12. Sensitivity analysis for structure for endogenous lyngbya mortality rate

Structural sensitivity analysis		
Structure	Setting 1	Setting 2
Effect LM coverage on mortality	With structure, exponential graph function	Without

With an exogenous mortality rate lyngbya biomass continues to grow after the initial sharp bloom. With the endogenous mortality rate lyngbya biomass declines after the initial bloom and settles into a new equilibrium around time 110. Endogenous effects on mortality appear to be important foci for further investigation. An endogenous mortality rate may give a more realistic picture of the dynamics of bloom limitation and may be of essence in further study focusing on the dynamics of bloom collapse.

Dissolved oxygen sector

Sensitivity of water residence and vertical mixing times *(normal water residence time* and *normal vertical mixing time)*

Water residence time is the average time for a given unit of water to be replaced by water from outside the study area. In our model we consider water outside the study area to be fully saturated. Vertical mixing time is the time required for water in the upper and lower water column to reach equilibrium for solutes, in our case dissolved oxygen and bioavailable iron. Both parameters are potentially important factors in the distribution of dissolved oxygen and bioavailable iron in the study area.

Water residence and vertical mixing times can vary greatly from one site to another. It is therefore of interest to examine the impact of these parameters on the lyngbya system behaviour through sensitivity analysis. It is very likely that water residence time and vertical mixing time are linked, therefore we conduct sensitivity of the parameters simultaneously. We conduct the sensitivity analysis on the water residence time of the lower water column as this will have the greater impact on lyngbya bloom.
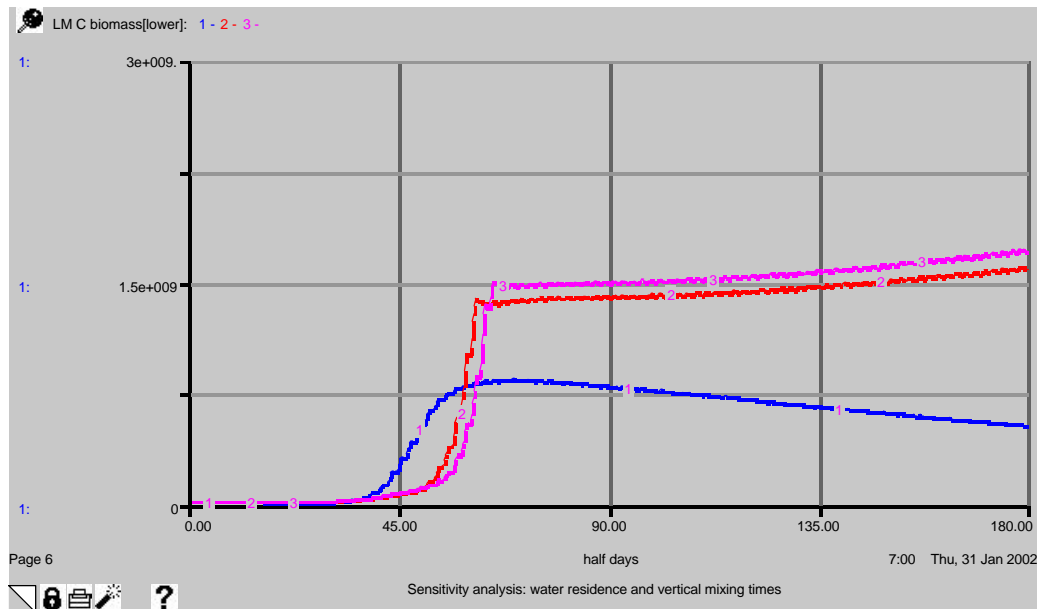

Figure 13. Sensitivity analysis of normal water residence and vertical mixing times

Parameter settings for sensitivity analysis (days)			
Parameter	Setting 1	Setting 2 (base)	Setting 3
Normal water residence time (lower)	.25	5	10
Normal vertical mix time	.25	2	5

When water residence time is set extremely low, as in setting 1, lyngbya bloom is greatly diminished because iron complex is available for a shorter period of time. The quantity of lyngbya biomass is not adequate to cause efflux of Fe2 from the sediments and the bloom is not sustained. This is consistent with field observations that areas with quick water turnover are not subject to lygnba blooms. It is surprising that lyngbya bloom initiates more quickly with the water exchanges times set with lower values. This occurs because faster water exchange pulls the iron concentration down to a level more optimal for carbon uptake. With slower exchange the level of bioavailable iron from the initial pulse of Fe complex may be above the optimal level, in a range inhibitory for carbon uptake. Based on this sensitivity analysis, we conclude that water exchange effects are likely to be of secondary importance to respiration and detritus decay.

Structure for effect of lyngbya coverage on water residence and vertical mixing times

When lyngbya blooms, thick matts of filamentous lyngbya tissue form on the benthic surface. These matts may restrict water exchange at the sediment-water interface. It is believed that this restricted water exchange may contribute to anoxic conditions at night. We have added a graph function *effect of LM coverage* to represent the impact of increasing density of lyngbya on water exchange and vertical mixing. In our model the non-linear function is s-shaped. At maximum density the water residence and vertical mixing times are increased by a factor of 10. For water residence time the effect only applies to the lower water column.
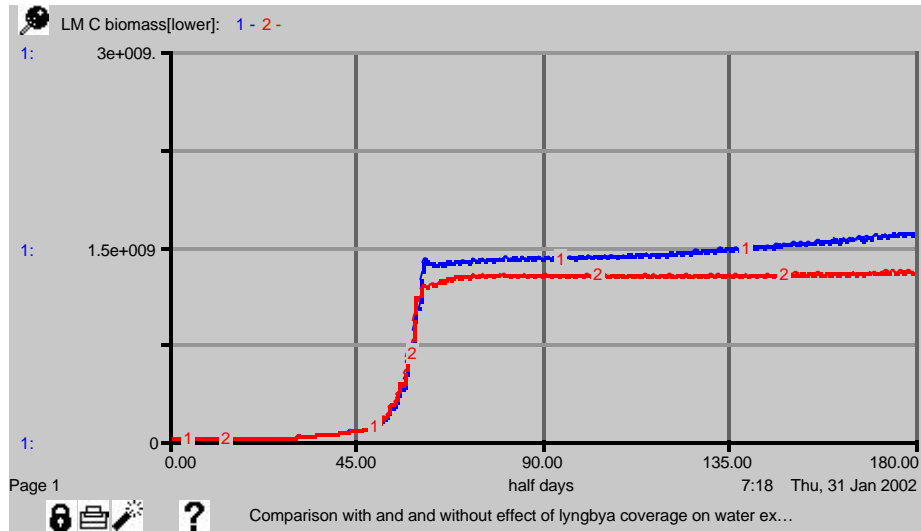
Figure 14. Sensitivity analysis for effect of lyngbya coverage on water exchange

Structural sensitivity analysis		
Structure	Setting 1 (base)	Setting 2
Effect of LM coverage on water exchange	With	Without

Simulation 1 has the structure in place for an effect of lyngbya coverage on water exchange (vertical mixing and water residence times). The lengthier mixing and residence times increase the availability of Fe2 allowing lyngbya biomass to continue growth after the initial sharp growth based on Fe complex. Setting 2 is run without the structure in place, lyngbya biomass is sustained without further increase. We conclude that water exchange restriction brought about by lyngbya growth may be an important factor contributing to Fe2 efflux at the sediment-water interface, but as in the case of water exchange, may be overshadowed in importance by respiration and detritus decay rates.

The Iron Sector

Decay rate of iron complex

We assume that the organically-bound iron complexes which we categorize as Fe complex will decay over time. However, the half-life of this decay and its links to other factors such as oxygen content are unknown. In the sensitivity analysis below we experiment with a range of decay times in order to observe the impact on lyngbya biomass growth.
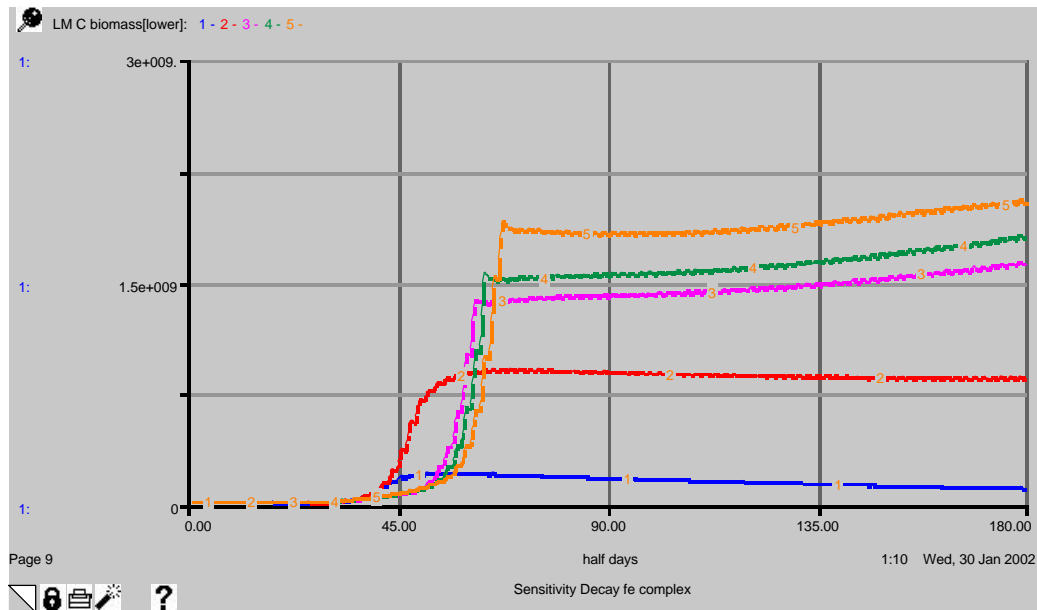

Figure 15. Sensitivity analysis of decay time for iron complex

Parameter setting for sensitivity analysis (days)				
Parameter	Setting 1	Setting 2	Setting 3	Setting 4	Setting 5
Decay time Fe complex	.25	1	10	20	100

In the simulation based on setting 1 there is inadequate bioavailable iron for lyngbya bloom to occur. Setting 2 allows lyngbya bloom to occur with adequate biomass to allow adequate Fe2 efflux to sustain the bloom. Overall the simulation results demonstrate a correlation between decay time and the initial growth rate of lyngbya. More rapid iron complex decay based on shorter decay times brings the level of bioavailable iron into the optimal range for growth. Whereas higher decay time settings lead to slower growth (because the bioavailable iron concentration is above the optimum range) but result in a larger stock of Fe complex on which to continue growth. The stability of the bioavailable organically-bound iron compounds is a pivotal issue in supporting or refuting our hypothesis of lyngbya bloom causation. Fe complex decay time is a key parameter for further research.

Reintroduction of iron through detritus decay

Iron will be released back to the environment by detritus decay. The extent to which this reintroduced iron is bioavailable is unknown. There is speculation that reintroduced iron may help sustain lyngbya blooms. In our model we assume that bioavailable reintroduced iron is organically bound and include it in the category Fe complex. We adjust the parameter determining bioavailability *fraction reintroduced Fe bioavail* in the following sensitivity analysis.
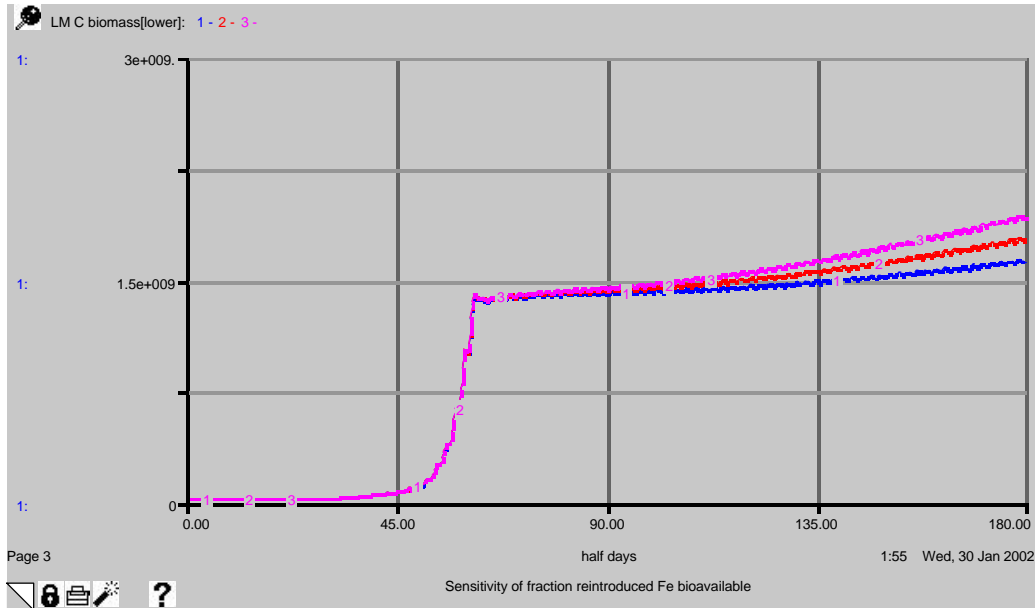
Figure 16. Sensitivity of bioavailability of reintroduced iron with Fe2 in sediment porewater

Parameter settings for sensitivity analysis (fraction, dimensionless)			
Parameter	Setting 1 (base)	Setting 2	Setting 3
Fraction reintroduced Fe bioavailable	0	.5	1
Conc Fe2 in porewater	5	5	5

As expected a higher fraction of bioavailability of reintroduced iron results in greater lyngbya growth. An alternative explanation for the persistence of lyngbya bloom could be that reintroduced bioavailable iron rather than Fe2 from sediment efflux sustains the bloom. We now re-run the simulation with Fe2 efflux set to zero.
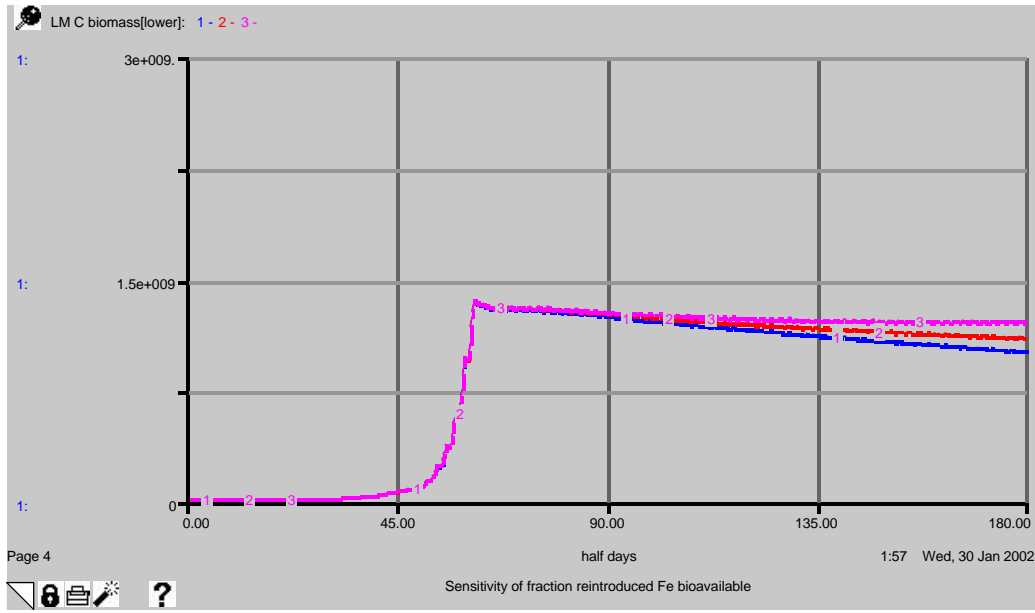
Figure 17. Sensitivity analysis for bioavailability of reintroduced iron with no Fe2 in sediment porewater.

Parameter settings for sensitivity analysis (fraction, dimensionless)			
Parameter	Setting 1 (base)	Setting 2	Setting 3
Fraction reintroduced Fe bioavailable	0	.5	1
Conc Fe2 in porewater	0	0	0

The higher fractions of bioavailability increase the sustainability of the bloom when there is no availability of Fe2. Reintroduced iron is lost from the system through water exchange and decay (another very uncertain parameter). If bioavailable iron is recyclable through detritus decay then reintroduced iron may sustain lyngbya blooms to a great extent if water residence time and decay time are relatively lengthy. It follows that the bioavailability of iron released from decaying detritus is a pertinent focus for empirical research.

Concentration of Fe2 in sediment porewater

The concentration of Fe2 in the sediment porewater is a key parameter in our hypothesis of lyngbya bloom. Fe2 efflux is directly proportional to the gradient of Fe2 concentration in the water column and in the porewater. If Fe2 porewater concentration is insufficient there will be inadequate Fe2 efflux to sustain the lyngbya bloom. Fe2 sediment concentration is an uncertain parameter which can vary greatly. We have no empirical data on the concentrations of Fe2 in our study areas. In the following sensitivity analysis we experiment with a range of values.
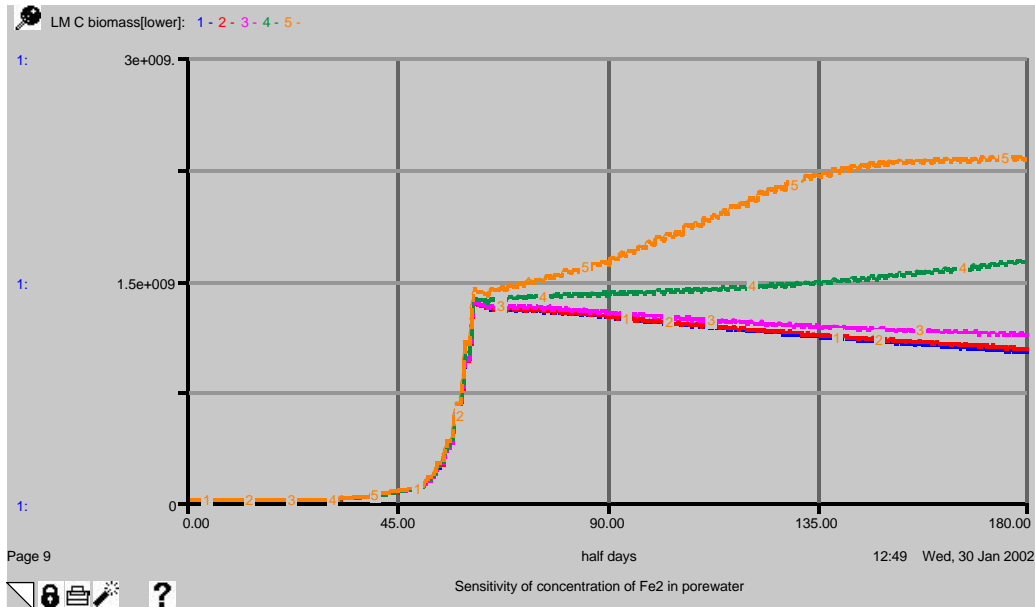
Figure 18. Sensitivity analysis of concentration of Fe2 in sediment porewater

Parameter setting for sensitivity analysis (grams m^{-3})				
Parameter	Setting 1	Setting 2	Setting 3	Setting 4	Setting 5
Conc Fe2 in porewater	0	.1	1	5 (base)	10

When Fe2 concentration is set at zero (setting 1) there is no efflux and the bloom is not sustained. Bloom growth is not sustained at settings 2 or 3. Setting 5 results in efflux which allows lyngbya biomass to reach its carrying capacity by time 180. Fe2 concentration in sediment porewaters is clearly an important focus for investigation. There are, however, other important factors in Fe2 efflux such as bioturbation which we consider in the next analysis.

Bioturbation factor

Bioturbation, the collective churning of sediments by benthic organisms, can significantly influence solute efflux from sediment porewaters (DiToro 2001). In our model bioturbation is represented as a multiplier which modifies the diffusion coefficient for Fe2. In the analysis that follows we observe the effects of a range of values for bioturbation.
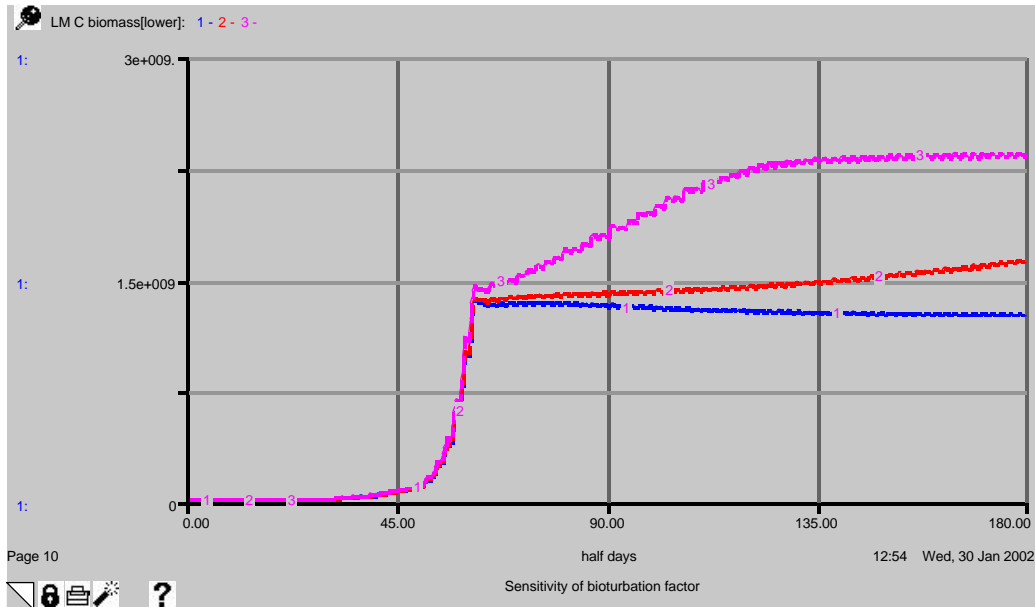
Figure 19. Sensitivity for bioturbation factor

Parameter setting for sensitivity analysis (multiplier, dimensionless)			
Parameter	Setting 1	Setting 2 (base value)	Setting 3
Bioturbation factor	1	2	5

At setting 1 (no bioturbation effect) the Fe2 efflux is insufficient to sustain the bloom. Setting of 5 results in rapid growth of lyngbya to its carrying capacity. Sensitivity analysis demonstrates that bioturbation has an important influence on the system behaviour. Given the importance and the uncertainty of this parameter, it is considered an important topic for investigation.

Seagrass Sector

Seagrass mortality

Investigations indicate that seagrass may be adversely impacted by lyngbya overgrowth through a shading effect. In our base simulation lyngbya coverage mimics a shading effect by decreasing seagrass carbon uptake. The seagrass mortality rate is exogenous. We compare the base simulation with a case in which seagrass mortality is effected by lyngbya coverage. The effect of lyngbya coverage on mortality could be interpreted as due to prolonged shading, toxic effects, or anoxia.
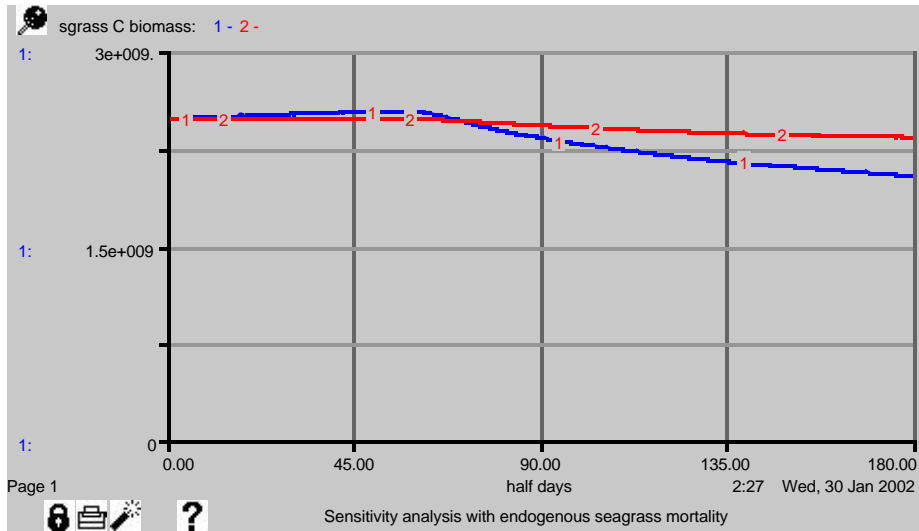
Figure 20. Sensitivity analysis for effect of lyngbya on seagrass mortality rate

Structural sensitivity analysis		
Structure	Setting 1	Setting 2 (base)
Effect LM coverage on seagrass mortality	With structure	Without

The base simulation with exogenous seagrass mortality suggest that the impact of lyngbya on seagrass is not extreme. The alternative simulation, with an endogenous seagrass mortality rate, produces a more readily apparent adverse impact. More empirical research is called for to measure the correlation between lyngbya density and duration of coverage with seagrass reduction through inhibition of growth and effects on mortality rates.

Summary and conclusion

The model described in this paper is for scoping and concensus building, the first stage of the three-stage modelling process proposed by Costanza and Ruth (1997). In our first stage model we have articulated an initial dynamic hypothesis to explain the occurrence of harmful blooms of Lyngbya Majuscula. The hypothesis draws on the work of scientists from a number of disciplines. Many of the parameters and structures of the model are uncertain. Through sensitivity analysis we have explored the implications of a number of these parameters and structures. Based on findings we have made suggestions for further research.

The first stage model has helped us identify specific research questions which may in some instances be addressed through field or laboratory work. These questions fall into two broad categories, those that are parametric and quantitative and those that are structural and qualitative in nature. Examples of the former are the maximum rate of carbon uptake and the respiration rate of lyngbya. These rates are not known with precision yet they are sensitive to system behaviour and central to model formulations. The first stage model also opens questions regarding model structures which have implications for understanding the system behaviour. For example, modelling lyngbya mortality as an endogenous variable versus an exogenous parameter prompts us ask a new set of questions regarding the relationships

between mortality, bloom dynamics and growth limitation. These questions can be explored through the development of more realistic and refined model structures.

The development of a second stage research model will be furthered by more accurate knowledge of key parameters and more realistic model structure. As we move into the second stage of modelling it is possible that aspects of our hypothesis will be refuted and alternative explanations adopted. Our goal is the development of a third stage management model which is well grounded scientifically and generally accepted by stakeholders involved with the lyngbya bloom problem.

Appendix
Model equations by sector

Lyngbya Majuscula (LM) Sector

LM_C_biomass[upper](t) = LM_C_biomass[upper](t - dt) + (LM_C_uptake[upper] + float_to_surface[upper] - LM_respiration[upper] - LM_mortality[upper,upper] - LM_mortality[upper,lower] - float_from_bottom[upper] - LM_biomass_loss__thru_drift[upper]) * dt
INIT LM_C_biomass[upper] = 0

LM_C_biomass[lower](t) = LM_C_biomass[lower](t - dt) + (LM_C_uptake[lower] + float_to_surface[lower] - LM_respiration[lower] - LM_mortality[lower,upper] - LM_mortality[lower,lower] - float_from_bottom[lower] - LM_biomass_loss__thru_drift[lower]) * dt
INIT LM_C_biomass[lower] = 1e7

INFLOWS:
LM_C_uptake[upper] = (IF (day_night_switch >=1) THEN
LM_C_biomass[upper]*C_uptake_rate_LM[upper] ELSE 0)
LM_C_uptake[lower] = (IF (day_night_switch >=1) THEN
LM_C_biomass[lower]*C_uptake_rate_LM[lower] ELSE 0)
float_to_surface[upper] = float_from_bottom[lower]
float_to_surface[lower] = float_from_bottom[lower]*0
OUTFLOWS:
LM_mortality[upper,upper] = LM_C_biomass[upper]*(LM_biomass_mortality_rate/2)
LM_mortality[upper,lower] = LM_C_biomass[upper]*(LM_biomass_mortality_rate)*0
LM_mortality[lower,upper] = LM_C_biomass[lower]*LM_biomass_mortality_rate*0
LM_mortality[lower,lower] = LM_C_biomass[lower]*(LM_biomass_mortality_rate/2)
LM_respiration[upper] = (IF day_night_switch<1 THEN
LM_C_biomass[upper]*LM_respiration_rate[upper] ELSE 0)
LM_respiration[lower] = (IF day_night_switch<1 THEN
LM_C_biomass[lower]*LM_respiration_rate[lower] ELSE 0)
float_from_bottom[upper] = LM_C_biomass[upper]*float_frac*0
float_from_bottom[lower] = LM_C_biomass[lower]*float_frac
LM_biomass_loss__thru_drift[upper] =
LM_C_biomass[upper]/(time_for__loss_thru_drift[upper]*2)
LM_biomass_loss__thru_drift[lower] =
(LM_C_biomass[lower]/time_for__loss_thru_drift[lower]*2)*0

LM_C_detritus[upper](t) = LM_C_detritus[upper](t - dt) + (LM_mortality[upper,upper] + LM_mortality[lower,upper] + settle_to_bottom[upper] - LM_detritus_decay[upper] - settle_fm_surface[upper] - LM_detritus_loss__thru_drift[upper]) * dt
INIT LM_C_detritus[upper] = 0

LM_C_detritus[lower](t) = LM_C_detritus[lower](t - dt) + (LM_mortality[upper,lower] + LM_mortality[lower,lower] + settle_to_bottom[lower] - LM_detritus_decay[lower] - settle_fm_surface[lower] - LM_detritus_loss__thru_drift[lower]) * dt
INIT LM_C_detritus[lower] = LM_C_biomass[lower]

INFLOWS:
LM_mortality[upper,upper] = LM_C_biomass[upper]*(LM_biomass_mortality_rate/2)
LM_mortality[upper,lower] = LM_C_biomass[upper]*(LM_biomass_mortality_rate)*0
LM_mortality[lower,upper] = LM_C_biomass[lower]*LM_biomass_mortality_rate*0
LM_mortality[lower,lower] = LM_C_biomass[lower]*(LM_biomass_mortality_rate/2)
settle_to_bottom[upper] = settle_fm_surface[upper]*0
settle_to_bottom[lower] = settle_fm_surface[upper]
OUTFLOWS:
LM_detritus_decay[upper] =
LM_C_detritus[upper]*LM_detritus_aerobic_decay_rate[upper]
LM_detritus_decay[lower] =
LM_C_detritus[lower]*LM_detritus_aerobic_decay_rate[lower]
settle_fm_surface[upper] = LM_C_detritus[upper]/(settling_time*2)
settle_fm_surface[lower] = (LM_C_detritus[lower]/(settling_time*2))*0
LM_detritus_loss__thru_drift[upper] =
LM_C_detritus[upper]/(time_for__loss_thru_drift[upper]*2)
LM_detritus_loss__thru_drift[lower] =
(LM_C_detritus[lower]/(time_for__loss_thru_drift[lower]*2))*0
carrying_capacity = total_area*max_density_LM*percent_C_of_dry_wt
C_uptake_rate_LM[upper] =
(max_C_uptake_rate_LM*(effect_density_on_C_fix/effect_density_on_C_fix)*effect_bioavail_Fe__on_C_uptake[upper])
C_uptake_rate_LM[lower] =
(max_C_uptake_rate_LM*effect_density_on_C_fix*effect_bioavail_Fe__on_C_uptake[lower])
day_night_switch = 1+SINWAVE(1,2)
density_LM = total_dwt_biomass/total_area
DO_limitation_factor[upper] = DO[lower]/DO_saturation_point
DO_limitation_factor[lower] = DO[lower]/DO_saturation_point
float_frac = max_float_frac*effect_photo__rate_on_float
LM_biomass_mortality_rate = .01
LM_coverage = (density_LM/max_density_LM)
LM_detritus_aerobic_decay_rate[upper] =
(normal_LM__detritus_decay_frac/2)*DO_limitation_factor[upper]
LM_detritus_aerobic_decay_rate[lower] =
normal_LM__detritus_decay_frac*DO_limitation_factor[lower]
LM_net_prod[upper] = DELAY (LM_C_uptake[upper],1)-LM_respiration[upper]
LM_net_prod[lower] = DELAY (LM_C_uptake[lower],1)-LM_respiration[lower]
LM_respiration_rate[upper] = DO_limitation_factor[upper]*normal_LM__respiration_rate
LM_respiration_rate[lower] = DO_limitation_factor[lower]*normal_LM__respiration_rate

max_C_uptake_rate_LM = .5
max_density_LM = 500
max_float_frac = .01/2
normal_LM__detritus_decay_frac = .01
normal_LM__respiration_rate = .01
percent_C_of_dry_wt = .4
settling_time = 1
time_for__loss_thru_drift[upper] = 10
time_for__loss_thru_drift[lower] = 60
total_area = 1e7
total_dwt_biomass =
(LM_C_biomass[upper]+LM_C_biomass[lower])/percent_C_of_dry_wt
total_LM_C_biomass = LM_C_biomass[lower] + LM_C_biomass[upper]
effect_bioavail_Fe__on_C_uptake[DO2] = GRAPH(bioavail_Fe[DO2])
(0.00, 0.00), (10.0, 0.00), (20.0, 0.00), (30.0, 0.00), (40.0, 0.00), (50.0, 0.00), (60.0, 0.00),
(70.0, 0.00), (80.0, 0.00), (90.0, 0.00), (100, 0.00)
effect_density_on_C_fix = GRAPH(LM_coverage)
(0.00, 1.00), (0.1, 1.00), (0.2, 1.00), (0.3, 1.00), (0.4, 0.99), (0.5, 0.955), (0.6, 0.915), (0.7,
0.82), (0.8, 0.66), (0.9, 0.365), (1, 0.001)
effect_photo__rate_on_float =
GRAPH(C_uptake_rate_LM[lower]/max_C_uptake_rate_LM)
(0.00, 0.00), (0.1, 0.00), (0.2, 0.00), (0.3, 0.00), (0.4, 0.00), (0.5, 0.02), (0.6, 0.06), (0.7, 0.21),
(0.8, 0.46), (0.9, 0.975), (1, 1.00)

Dissolved Oxygen (DO) Sector

DO[upper](t) = DO[upper](t - dt) + (DO_replenishment[upper] + DO_fm_air[upper] +
verticle_DO_exchange_in[upper] - DO_consumption[upper] -
DO_release_to_atmosphere[upper] - verticle_DO_exchange_out[upper]) * dt
INIT DO[upper] = DO_saturation_point

DO[lower](t) = DO[lower](t - dt) + (DO_replenishment[lower] + DO_fm_air[lower] +
verticle_DO_exchange_in[lower] - DO_consumption[lower] -
DO_release_to_atmosphere[lower] - verticle_DO_exchange_out[lower]) * dt
INIT DO[lower] = DO_saturation_point

INFLOWS:
DO_replenishment[upper] =
DO_replenishment_thru_mixing[upper]+DO_replenish_thru_LM_C_fix[upper]+(DO_replen
ish_thru_sgrass_C_fix*0)
DO_replenishment[lower] =
DO_replenishment_thru_mixing[lower]+DO_replenish_thru_LM_C_fix[lower]+DO_repleni
sh_thru_sgrass_C_fix
DO_fm_air[upper] = (IF (diff_saturation_&_DO[upper]>0) THEN
(diff_saturation_&_DO[upper]/time_to_sat_frm_atmosphere) ELSE 0)
DO_fm_air[lower] = (diff_saturation_&_DO[lower]/time_to_sat_frm_atmosphere)*0
verticle_DO_exchange_in[upper] = verticle_DO_exchange_out[lower]
verticle_DO_exchange_in[lower] = verticle_DO_exchange_out[upper]
OUTFLOWS:

DO_consumption[upper] =
((DO_consumption_thru_LM_respiration[upper]+DO_consumption_thru_LM_detritus_deca
y[upper]+(DO_consumption_thru_sgarss_detritus_decay*0)+(DO_consumption_thru_sgrass
_respiration*0))/water_vol_per_layer)+consumption_DO_thru_Fe2_precip[upper]
DO_consumption[lower] =
((DO_consumption_thru_LM_detritus_decay[lower]+DO_consumption_thru_LM_respiratio
n[lower]+DO_consumption_thru_sgarss_detritus_decay+DO_consumption_thru_sgrass_resp
iration)/water_vol_per_layer)+consumption_DO_thru_Fe2_precip[lower]
DO_release_to_atmosphere[upper] = IF (diff_saturation_&_DO[upper]< 0) THEN
(DO_replenishment[upper]+verticle_DO_exchange_in[upper]) ELSE 0
DO_release_to_atmosphere[lower] = (IF (diff_saturation_&_DO[lower]< 0) THEN
(DO_replenishment[lower]+verticle_DO_exchange_in[lower]) ELSE 0)*0
verticle_DO_exchange_out[upper] =
(diff_DO_upper_&_lower[upper]/2)/vert_mix_time[upper]+diff_saturation_&_DO[upper]*0
+DO_replenishment[upper]*0
verticle_DO_exchange_out[lower] = IF (diff_saturation_&_DO[lower]>=0) THEN
(diff_DO_upper_&_lower[lower]/2)/vert_mix_time[lower] ELSE
(diff_DO_upper_&_lower[lower]/2)/vert_mix_time[lower] + DO_replenishment[lower]
consumption_DO_thru_Fe2_precip[upper] = precip_Fe2[upper]*ratio_O_to_Fe
consumption_DO_thru_Fe2_precip[lower] = precip_Fe2[lower]*ratio_O_to_Fe
diff_DO_upper_&_lower[upper] = DO[upper]-DO[lower]
diff_DO_upper_&_lower[lower] = DO[lower]-DO[upper]
diff_saturation_&_DO[upper] = DO_saturation_point-DO[upper]
diff_saturation_&_DO[lower] = DO_saturation_point-DO[lower]
DO_consumption_thru_LM_detritus_decay[upper] =
LM_detritus_decay[upper]*wt_ratio_O_to_C
DO_consumption_thru_LM_detritus_decay[lower] =
LM_detritus_decay[lower]*wt_ratio_O_to_C
DO_consumption_thru_LM_respiration[upper] = LM_respiration[upper]*wt_ratio_O_to_C
DO_consumption_thru_LM_respiration[lower] = LM_respiration[lower]*wt_ratio_O_to_C
DO_consumption_thru_sgarss_detritus_decay = seagrass_detritus_decay*wt_ratio_O_to_C
DO_consumption_thru_sgrass_respiration = seagrass_respiration*wt_ratio_O_to_C
DO_replenishment_thru_mixing[upper] =
diff_saturation_&_DO[upper]/water_residence_time[upper]
DO_replenishment_thru_mixing[lower] =
diff_saturation_&_DO[lower]/water_residence_time[lower]
DO_replenish_thru_LM_C_fix[upper] =
(LM_C_uptake[upper]*wt_ratio_O_to_C)/water_vol_per_layer
DO_replenish_thru_LM_C_fix[lower] =
(LM_C_uptake[lower]*wt_ratio_O_to_C)/water_vol_per_layer
DO_replenish_thru_sgrass_C_fix =
(seagrass__C_uptake*wt_ratio_O_to_C)/water_vol_per_layer
DO_saturation_point = 7
normal_vert_mix_time = 2
normal_water_residence_time[upper] = 5
normal_water_residence_time[lower] = 5.25
ratio_O_to_Fe = .57
time_to_sat_frm_atmosphere = 4
vert_mix_time[DO2] =
(normal_vert_mix_time*2)*effect_LM_coverage_on_water_exchange

water_residence_time[upper] =
(normal_water_residence_time[upper]*2)*(effect_LM_coverage_on_water_exchange/effect_
LM_coverage_on_water_exchange)
water_residence_time[lower] =
(normal_water_residence_time[lower]*2)*effect_LM_coverage_on_water_exchange
wt_ratio_O_to_C = 2.67
effect_LM_coverage_on_water_exchange = GRAPH(LM_coverage)
(0.00, 1.00), (0.1, 1.00), (0.2, 1.00), (0.3, 1.23), (0.4, 1.77), (0.5, 2.80), (0.6, 6.40), (0.7, 8.65),
(0.8, 9.55), (0.9, 9.82), (1, 10.0)

[1]*Iron (Fe) Sector*

Fe2[upper](t) = Fe2[upper](t - dt) + (efflux_Fe2[upper] + Fe2_vert_mix_in[upper] -
precip_Fe2[upper] - Fe2_uptake[upper] - loss_Fe2_due_mixing[upper] -
Fe2_vert_mix_out[upper]) * dt
INIT Fe2[upper] = 0

Fe2[lower](t) = Fe2[lower](t - dt) + (efflux_Fe2[lower] + Fe2_vert_mix_in[lower] -
precip_Fe2[lower] - Fe2_uptake[lower] - loss_Fe2_due_mixing[lower] -
Fe2_vert_mix_out[lower]) * dt
INIT Fe2[lower] = 0

INFLOWS:
efflux_Fe2[upper] = indicated_Efflux_Fe2*effect_of_DO_on_efflux*0
efflux_Fe2[lower] = (indicated_Efflux_Fe2*effect_of_DO_on_efflux)/2
Fe2_vert_mix_in[upper] = Fe2_vert_mix_out[lower]
Fe2_vert_mix_in[lower] = Fe2_vert_mix_out[upper]
OUTFLOWS:
precip_Fe2[upper] = Fe2[upper]/(MAX(Fe2_precip_time[upper],DT*3))
precip_Fe2[lower] = Fe2[lower]/(MAX (Fe2_precip_time[lower],DT*3))
Fe2_uptake[upper] = uptake_bioavail_Fe[upper]*Fe2_to_bioavail_Fe[upper]
Fe2_uptake[lower] = uptake_bioavail_Fe[lower]*Fe2_to_bioavail_Fe[lower]
loss_Fe2_due_mixing[upper] = (Fe2[upper]/water_residence_time[upper])
loss_Fe2_due_mixing[lower] = (Fe2[lower]/water_residence_time[lower])
Fe2_vert_mix_out[upper] = ((diff_Fe2_upper&lower[upper]/2)/vert_mix_time[upper])
Fe2_vert_mix_out[lower] = ((diff_Fe2_upper&lower[lower])/2)/vert_mix_time[lower])
Fe__complex[upper](t) = Fe__complex[upper](t - dt) + (inflow_Fe_complex[upper] +
Fe_reintroduction[upper] + Fe_comp_vert_mix_in[upper] - decay__Fe_complex[upper] -
loss_Fe_complex__due_lateral_mixing[upper] - Fe_complex__uptake[upper] -
Fe_comp_vert_mix_out[upper]) * dt
INIT Fe__complex[upper] = .1

Fe__complex[lower](t) = Fe__complex[lower](t - dt) + (inflow_Fe_complex[lower] +
Fe_reintroduction[lower] + Fe_comp_vert_mix_in[lower] - decay__Fe_complex[lower] -
loss_Fe_complex__due_lateral_mixing[lower] - Fe_complex__uptake[lower] -
Fe_comp_vert_mix_out[lower]) * dt
INIT Fe__complex[lower] = .1

INFLOWS:

inflow_Fe_complex[upper] = total_inflow_Fe_complex/water_vol_per_layer

inflow_Fe_complex[lower] = total_inflow_Fe_complex/water_vol_per_layer

Fe_reintroduction[upper] =
(((LM_detritus_decay[upper])*ratio_Fe_to_C)/water_vol_per_layer)*frac_reintroduced_Fe_
bioavail

Fe_reintroduction[lower] =
(((LM_detritus_decay[lower])*ratio_Fe_to_C)/water_vol_per_layer)*frac_reintroduced_Fe_
bioavail

Fe_comp_vert_mix_in[upper] = Fe_comp_vert_mix_out[lower]

Fe_comp_vert_mix_in[lower] = Fe_comp_vert_mix_out[upper]

OUTFLOWS:

decay__Fe_complex[Ferric_Fe] = Fe__complex[Ferric_Fe]/(decay_time_Fe_complex*2)

loss_Fe_complex__due_lateral_mixing[upper] =
Fe__complex[upper]/water_residence_time[upper]

loss_Fe_complex__due_lateral_mixing[lower] =
Fe__complex[lower]/water_residence_time[lower]

Fe_complex__uptake[upper] =
uptake_bioavail_Fe[upper]*Fe_complex_to_bioavail_Fe[upper]

Fe_complex__uptake[lower] =
Fe_complex_to_bioavail_Fe[lower]*uptake_bioavail_Fe[lower]

Fe_comp_vert_mix_out[upper] =
(diff_Fe_comp_upper&lower[upper]/2)/vert_mix_time[upper]

Fe_comp_vert_mix_out[lower] =
(diff_Fe_comp_upper&lower[lower]/2)/vert_mix_time[lower]

baseflow_Fe_complex = 150000

bioavail_Fe[upper] = Fe2[upper]+Fe__complex[upper]

bioavail_Fe[lower] = Fe2[lower]+Fe__complex[lower]

bioturbation_factor = 2.5

Conc_Fe2_in_pore_water = 5

decay_time_Fe_complex = 10

diffusion_coefficient = .7

Diff_conc_Fe2_sed__&_lower_water_column = (Conc_Fe2_in_pore_water-Fe2[lower])

diff_Fe2_upper&lower[upper] = Fe2[upper]-Fe2[lower]

diff_Fe2_upper&lower[lower] = Fe2[lower]-Fe2[upper]

diff_Fe_comp_upper&lower[upper] = Fe__complex[upper]-Fe__complex[lower]

diff_Fe_comp_upper&lower[lower] = Fe__complex[lower]-Fe__complex[upper]

dispersion_pulse_Fe_complex =
SMTH1(pulse_Fe_complex_from_rain_event,(dispersion_time*2))/2

dispersion_time = 3

Fe2_precip_time[DO2] = DO[DO2]/DO_saturation_point

Fe2_to_bioavail_Fe[upper] = IF Fe2[upper]>0 THEN Fe2[upper]/bioavail_Fe[upper] ELSE 0

Fe2_to_bioavail_Fe[lower] = IF Fe2[lower]>0 THEN Fe2[lower]/bioavail_Fe[lower] ELSE 0

Fe_complex_to_bioavail_Fe[upper] = IF Fe__complex[upper]>0 THEN
Fe__complex[upper]/bioavail_Fe[upper] ELSE 0

Fe_complex_to_bioavail_Fe[lower] = IF Fe__complex[lower]>0 THEN
Fe__complex[lower]/bioavail_Fe[lower] ELSE 0

frac_reintroduced_Fe_bioavail = 0

indicated_Efflux_Fe2 =
(Diff_conc_Fe2_sed__&_lower_water_column*porosity*(diffusion_coefficient*bioturbation
_factor))
porosity = .6
ratio_Fe_to_C = .05
total_inflow_Fe_complex = baseflow_Fe_complex+dispersion_pulse_Fe_complex
uptake_bioavail_Fe[upper] = IF LM_net_prod[upper]>0 THEN
(LM_net_prod[upper]*ratio_Fe_to_C)/water_vol_per_layer ELSE 0
uptake_bioavail_Fe[lower] = IF LM_net_prod[lower]>0 THEN
(LM_net_prod[lower]*ratio_Fe_to_C)/water_vol_per_layer ELSE 0
water_vol_per_layer = 1e7
effect_of_DO_on_efflux = GRAPH(DO[lower]/DO_saturation_point)
(0.00, 1.00), (0.1, 0.785), (0.2, 0.595), (0.3, 0.43), (0.4, 0.31), (0.5, 0.235), (0.6, 0.175), (0.7,
0.125), (0.8, 0.075), (0.9, 0.035), (1, 0.00)
Fe2_precip_time[DO2] = DO[DO2]/DO_saturation_point
pulse_Fe_complex_from_rain_event = GRAPH(TIME)
(0.00, 0.00), (1.00, 0.00), (2.00, 0.00), (3.00, 0.00), (4.00, 0.00), (5.00, 0.00), (6.00, 0.00),
(7.00, 0.00), (8.00, 0.00), (9.00, 0.00), (10.0, 0.00), (11.0, 0.00), (12.0, 0.00), (13.0, 0.00),
(14.0, 0.00), (15.0, 0.00), (16.0, 0.00), (17.0, 0.00), (18.0, 0.00), (19.0, 0.00), (20.0, 0.00),
(21.0, 0.00), (22.0, 0.00), (23.0, 0.00), (24.0, 0.00), (25.0, 0.00), (26.0, 0.00), (27.0, 0.00),
(28.0, 0.00), (29.0, 0.00), (30.0, 3.1e+008), (31.0, 3.1e+008), (32.0, 3e+008), (33.0, 0.00),
(34.0, 0.00), (35.0, 0.00), (36.0, 0.00), (37.0, 0.00), (38.0, 0.00), (39.0, 0.00), (40.0, 0.00),
(41.0, 0.00), (42.0, 0.00), (43.0, 0.00), (44.0, 0.00), (45.0, 0.00), (46.0, 0.00), (47.0, 0.00),
(48.0, 0.00), (49.0, 0.00), (50.0, 0.00), (51.0, 0.00), (52.0, 0.00), (53.0, 0.00), (54.0, 0.00),
(55.0, 0.00), (56.0, 0.00), (57.0, 0.00), (58.0, 0.00), (59.0, 0.00), (60.0, 0.00), (61.0, 0.00),
(62.0, 0.00), (63.0, 0.00), (64.0, 0.00), (65.0, 0.00), (66.0, 0.00), (67.0, 0.00), (68.0, 0.00),
(69.0, 0.00), (70.0, 0.00), (71.0, 0.00), (72.0, 0.00), (73.0, 0.00), (74.0, 0.00), (75.0, 0.00),
(76.0, 0.00), (77.0, 0.00), (78.0, 0.00), (79.0, 0.00), (80.0, 0.00), (81.0, 0.00), (82.0, 0.00),
(83.0, 0.00), (84.0, 0.00), (85.0, 0.00), (86.0, 0.00), (87.0, 0.00), (88.0, 0.00), (89.0, 0.00),
(90.0, 0.00), (91.0, 0.00), (92.0, 0.00), (93.0, 0.00), (94.0, 0.00), (95.0, 0.00), (96.0, 0.00),
(97.0, 0.00), (98.0, 0.00), (99.0, 0.00), (100, 0.00)

Seagrass Sector

sgrass_C_biomass(t) = sgrass_C_biomass(t - dt) + (seagrass__C_uptake - seagrass__turnover
- seagrass_respiration) * dt
INIT sgrass_C_biomass = ((total_area-
LM_coverage*total_area)*max_density_seagrass)/C_to_dwt_conv_seagrass

INFLOWS:
seagrass__C_uptake = IF (day_night_switch >=1) THEN
(sgrass_C_biomass*seagrass_C_uptake_rate) ELSE 0
OUTFLOWS:
seagrass__turnover = (sgrass_C_biomass*(seagrass_turnover_rate/2))
seagrass_respiration = IF day_night_switch<1 THEN
sgrass_C_biomass*seagrass_respiration_rate ELSE 0
sgrass_C_detritus(t) = sgrass_C_detritus(t - dt) + (seagrass__turnover -
seagrass_detritus_decay) * dt
INIT sgrass_C_detritus = sgrass_C_biomass

INFLOWS:
seagrass__turnover = (sgrass_C_biomass*(seagrass_turnover_rate/2))
OUTFLOWS:
seagrass_detritus_decay = (sgrass_C_detritus*seagrass_detritus_decay_rate)
C_to_dwt_conv_seagrass = 2
density_seagrass = total_dwt_seagrass/total_area
max_density_seagrass = 500
max_seagrass_C_uptake = .02
normal_seagrass_detritus_decay_rate = .69/seagrass_detritus_halflife
normal_seagrass_night_respiration_rate = .001
seagrass_C_uptake_rate =
max_seagrass_C_uptake*self_limiting_effect_of_seagrass_density_on_seagrass_C_uptake*s
hading_effect_of_lyngbya_on_seagrass
seagrass_detritus_decay_rate =
(DO_limitation_factor[lower]*normal_seagrass_detritus_decay_rate)/2
seagrass_detritus_halflife = 690
seagrass_respiration_rate =
normal_seagrass_night_respiration_rate*DO_limitation_factor[lower]
seagrass_turnover_rate = .001
total_dwt_seagrass = sgrass_C_biomass*C_to_dwt_conv_seagrass
self_limiting_effect_of_seagrass_density_on_seagrass_C_uptake =
GRAPH(density_seagrass/max_density_seagrass)
(0.00, 1.00), (0.1, 0.995), (0.2, 0.95), (0.3, 0.735), (0.4, 0.485), (0.5, 0.28), (0.6, 0.18), (0.7, 0.135), (0.8, 0.105), (0.9, 0.1), (1, 0.1)
shading_effect_of_lyngbya_on_seagrass = GRAPH(LM_coverage)
(0.00, 1.00), (0.1, 0.995), (0.2, 0.965), (0.3, 0.855), (0.4, 0.585), (0.5, 0.315), (0.6, 0.19), (0.7, 0.105), (0.8, 0.04), (0.9, 0.00), (1, 0.00)

References

Anderson, J.M. 1973. The Eutrophication of Lakes. In Toward Global Equilibrium, edited by Meadows, D. and D. Meadows. Cambridge MA: Wright-Allen Press.

Beer, S., W. Spencer, and G. Bowes. 1986. Photosynthesis and Growth of the Filamentous Blue-Green Alga *Lyngbya birgei* in Relation to its Environment. *Journal of Aquatic Plant Management*. 24: 61-65.

Costanza, R., M. Ruth. 1997. Dynamic Systems modelling for Scoping and Consensus Building. In *Sustainability and Global Environmental policy: New Perspectives*, edited by A.K. Dragun and K.M. Jakonson. Cheltenham, U.K. Edward Elgan.

Dennison, W.C., J.M. O'Neal, E.J. Duffy, P.E. Oliver, G.R. Shaw. 1999. Blooms of the Cyanobacterium Lyngbya majuscula in Coastal Waters of Queensland, Australia. *Bulletin de l'Institut Oceanographique, Monaco*. 19: 501-506.

DiToro, D. M. 2001. *Sediment Flux Modelling*. New York: Wiley.

Ford, Andrew. 1999. *Modeling the Environment: An Introduction to System Dynamics Modeling of Environmental Systems*. Washington D.C.: Island Press.

Gross, E.D. and D. Martin. 1996. Iron Dependence of Lyngbya majuscula. *Journal of Aquatic Plant Management*. 34: 17-20.

Hannon, B. and M. Ruth. 1997. *Modeling Dynamic Biological Systems*. New York: Springer.

Hewson, I., J.M. O'Neal, W.C. Dennison. 2001. Virus-like Particles Associated with Lyngbya majuscula (Cyanophyta, Oscillatoriacea) Bloom Decline in Moreton Bay, Australia. *Aquatic Microbial Ecology*. 25: 207-213.

Hemminga, Marten. A. and Carlos.M. Duarte. 2000. *Seagrass Ecology*. New York: Cambridge University Press.

Hoffman, P.A.G., de Jonge, S.A. Wagenvoort, E.J., and A.J.J. Sandee. 1991. Apparent sediment diffusion coefficients for oxygen consumption rates measured with microelectrodes and bell jars: applications to sediment oxygen budgets in esturine intertidal sediments. *Mar. Eco. Prog. Ser*. 69, 261-272.

Matsunaga, K., J. Nishioka, K. Kuma, K. Toya and Y. Suzuki. 1998. Riverine Input of Bioavailable Iron Supporting Phytoplankton Growth in Kesennuma Bay (Japan). *Water Research*. 32: 3436-3442.

Osborne, N.J.T., P. Webb, I. Stewart and G. Shaw. 2000. Human Toxicology and Epidemiology of the Marine Blue-Green Alga *Lyngbya Majuscula*. In *Proceedings of the Ninth Conference on Harmful Algal Blooms*. Hobart, Tasmania.

O'Neal, J.M., G.R. Shaw, W.C. Dennison. 2000. Blooms of the Toxic Cyanobacteria *Lyngbya Majuscula* in Costal Queensland Waters. In *Proceedings of the Ninth Conference on Harmful Algal Blooms*. Hobart, Tasmania.

Sterman, J. 2000. *Business Dynamics*. New York: Irwin/McGraw-Hill.

U.S. Environmental Protection Agency. 1985. *Rates, Constants, and Kinetics Formulations in Surface Water Quality Modelling* (2nd. Ed.) Lafayette, Ca.,Tetra Tech, Incorporated.

Watkinson, A. 2000. *Ecophysiology of the Marine Cyanobacterium, Lyngbya majuscula (Oscillatoriacea).* Brisbane, Australia, University of Queensland.